

UNIVERSITY OF OTTAWA  
MCG4322  
GROUP RE3  
WILDCAT DESIGN



---

## Capstone Report

---

**Volume  $x$  of  $y$**

Joey Kane - 7386330  
Isaak Goldenberg - 7395188  
Sawyer Woodside - 7158568  
Alex Pennell - 7334789

December 8, 2017



*Sponsor:* Dr. Eric Lanteigne



# Abstract

Volume 1 of the Capstone Report contains the main body of the report, including all design and analysis information. Volume 2 contains all appendices.

The aim of this design was to create a system for control of an unmanned airship. It was achieved by using a gondola as a ballast to move the centre of mass in relation to the centre of volume and initiate pitch changes. The design features stationary thrusters located in the XY plane of the airship, attached by carbon fibre arms which are secured to a pre-existing keel. The keel acts as a rail for the gondola to move back and forth on. The gondola contains control equipment used to communicate with the thruster assembly wirelessly, as well as drive the gondola to the desired position. Passive breaking is highly desirable and achieved through a linear actuator with a holding force with no signal. Vectoring of the propellers is achieved by a servo motor mounted to a plate which connects to the thruster arms.

The dimensions of the airship may vary as it is not manufactured yet, and input parameters are selected by the user, meaning that the whole airship must be scalable and feasible. A GUI is implemented in MATLAB to ensure that the user selects values which are feasible and produces SolidWorks Models that can be used as reference for manufacturing and design.

iv.Illustration of the final design????



# Contents

<b>1</b>	<b>Introduction</b>	<b>1</b>
1.1	Project Mandate . . . . .	1
1.2	Group Problem Scope . . . . .	1
1.3	Criteria and Restrictions . . . . .	1
1.4	Parametrization Overview . . . . .	1
<b>2</b>	<b>Analysis</b>	<b>3</b>
2.1	Outline . . . . .	3
2.2	High Level Parametrization . . . . .	4
2.3	System Modelling . . . . .	4
2.3.1	Thrusters . . . . .	4
2.3.2	Gondola Forces . . . . .	4
2.3.3	Loading Scenarios . . . . .	6
2.3.4	Drag Analysis . . . . .	6
2.3.5	Envelope Analysis . . . . .	9
2.4	Component Analysis . . . . .	9
2.4.1	Thruster Assembly Component Selection . . . . .	9
2.4.2	Thruster Shaft . . . . .	9
2.4.3	Thruster Arms . . . . .	11
2.4.4	Connection To Keel . . . . .	12
2.4.5	Friction Wheel Slip . . . . .	13
2.4.6	Bolt Compression Force . . . . .	16
2.4.7	Linear Actuator . . . . .	19
2.4.8	Gondola Arm Stresses . . . . .	21
2.4.9	Bearing Mounting (Snap-Fit) . . . . .	24
<b>3</b>	<b>Discussion</b>	<b>27</b>
<b>A</b>	<b>Instructions for Installing and Running the GUI</b>	<b>35</b>
<b>B</b>	<b>Code</b>	<b>37</b>
B.1	Code 1 . . . . .	37
<b>C</b>	<b>Additional Material</b>	<b>43</b>
C.1	Gondola Arm Deflection . . . . .	43
C.2	Gondola Arm Fatigue Failure . . . . .	43

C.3 Thruster Arm Adhesion . . . . .	45
C.4 Gondola Motor Shaft . . . . .	47
C.5 Vectoring Shaft Screw Axial Loading Conditions . . . . .	47
C.6 Vectoring Motor . . . . .	48
C.7 Gondola Hinge . . . . .	49
C.8 Bearings . . . . .	50
C.8.1 Gondola Bearings . . . . .	50
C.8.2 Thruster Bearings . . . . .	50
C.8.3 Thruster Bearings Press Fit . . . . .	50
C.9 Cauchy Stress Tensor [33] . . . . .	52
C.10 Thrust Force . . . . .	53
C.11 Previous Drag Analysis . . . . .	60
<b>D Data Sheets</b>	<b>63</b>
D.1 Material Properties . . . . .	63
D.1.1 3D Printed Nylon 12 [31] . . . . .	63
D.2 Linear Actuator [1] . . . . .	65
D.3 Bearings [21] . . . . .	66
D.4 Friction Wheel Assembly . . . . .	67
D.4.1 Friction Wheel [20] . . . . .	67
D.4.2 Friction Wheel Set Screw [22] . . . . .	68
D.4.3 Friction Wheel Motor [25] . . . . .	69
D.4.4 Friction Wheel Encoder [26] . . . . .	71
D.4.5 Example Cable Gland [18] . . . . .	72
D.5 Keel Construction Quote . . . . .	74
D.6 Spring [23] . . . . .	75
D.7 Battery [9] . . . . .	76
D.8 Thruster Assembly . . . . .	77
D.8.1 Thruster Motor [16] . . . . .	77
D.8.2 Propeller [14] . . . . .	78
D.8.3 BESC [10] . . . . .	79
D.8.4 Servo Motor [27] . . . . .	80
D.8.5 Receiver [15] . . . . .	82
D.9 Flight Control Assembly . . . . .	83
D.9.1 ESC [11] . . . . .	83
D.9.2 GPS Module [13] . . . . .	84
D.9.3 Transceiver [17] . . . . .	85

D.9.4 Flight Controller [12] . . . . .	86
<b>E Engineering Drawings</b>	<b>87</b>
E.1 Parts List . . . . .	87
E.2 Complete System Drawing . . . . .	87
E.3 Sub-Assembly Drawings . . . . .	87
E.4 Individual Part Drawings . . . . .	87
<b>F Meeting Minutes</b>	<b>89</b>
F.1 Group Meeting Minutes . . . . .	89
F.2 Team-Partner Meeting Minutes . . . . .	101
<b>G Recommendations for Improving the Course</b>	<b>103</b>



# List of Figures

1.1	Overview of Modelling Parametrization	2
2.1	Parametrization Outline for the Thruster Shaft	9
2.2	Parametrization Outline for the Thruster Arms	11
2.3	Parametrization Outline for the Thruster Arm Connector	12
2.4	Parametrization Outline for the Friction Wheel Slip	13
2.5	Parametrization Outline for the Bolt Compression Force	16
2.6	Parametrization Outline for the Bolt Compression	19
2.7	Parametrization Outline for the Gondola Arms	21
2.8	Model Used to Compute the Deflection of the Gondola Arms	22
2.9	Parametrization Outline of Snapfit Analysis	24
2.10	Centeroid of Section of Circle [34]	25
C.1	S-N Curve for Laser Sintered Nylon [3], Used to Determine the Fatigue Failure of the Gondola Body	44
C.2	Analysis of Carbon Fibre Adhesion (From Shigley's Machine Design [5, 484])	45
C.3	HS-7950TH Servo Spline Attachment [28]	47
C.4	Thruster Pitching Shaft Worst Case Moment of Inertia	49
C.5	Gondola Hinge Comparison Fillet Vs. No Fillet	50
C.6	Pressfit Interference Diameters [7]	51
C.7	Graph of Thrust Plotted Against Airship Speed at 11000rpm With 7", 5" Pitch Diameter Propeller	56
C.8	Test Data from Gabriel Staples Against Experimental Static Thrust Values [30]	57
C.9	Test Data from Gabriel Staples Against Experimental Dynamic Thrust Values [30]	58
C.10	Sample Thrust Calculation Using On-line Calculator [8]	59
C.11	Drag Force Curves Computed From SolidWorks Flow Simulation	60
C.12	Drag Force Curves Computed From SolidWorks Flow Simulation	61



# List of Tables

2.1	List of All Parametrized Components . . . . .	3
2.2	List of All Inconsequential Analysis . . . . .	3
2.3	Airship Model Characteristics and Data [32] Continued . . . . .	7
2.4	Drag Contribution for Various Airship Components [32] . . . . .	8
2.5	Fineness Ratios and Corresponding $C_D$ . . . . .	8
C.1	Table of Bolt Strength for a M3-0.5 Bolt [2] . . . . .	48
C.2	Table of Calculated Thrust Values for Varying Airship Speeds . . . . .	55
C.3	Raw Data From SolidWorks Flow Simulation . . . . .	60
D.1	Various Gearing For Gondola Motor Torque [25]. . . . .	70



# Nomenclature

$E_p$	Modulus of elasticity of considered plastic hub or boss [ $N/mm^2$ ]
$F_R$	Keel to assembly arm connector reaction, [ $N$ ]
$F_T$	Thruster force, [ $N$ ]
$F_g$	Force of gravity, [ $N$ ]
$F_{GR}$	Reaction force of gondola, [ $N$ ]
$F_{K1}$	Keel reaction force 1, [ $N$ ]
$F_{K2}$	Keel reaction force 2, [ $N$ ]
$F_{LA}$	Linear actuator force, [ $N$ ]
$F_{NB}$	Normal force applied to bearing, [ $N$ ]
$F_{RSF}$	Force of snap fit bearing [ $N$ ]
$F_\alpha$	Force on fastener $\alpha$ (hinge to gondola), [ $N$ ]
$F_\beta$	Force on fastener $\beta$ (hinge to gondola), [ $N$ ]
$F_a$	Force on fastener a (hinge to gondola), [ $N$ ]
$F_{bolt}$	Bolt pretension force, [ $N$ ]
$F_{brake}$	Normal braking force keel reaction, [ $N$ ]
$F_b$	Force on fastener b (hinge to gondola), [ $N$ ]
$F_{c1}$	Connector moment couple force 1, [ $N$ ]
$F_{c2}$	Connector moment couple force 2, [ $N$ ]
$F_{ffric}$	Friction force acting on friction wheel, [ $N$ ]
$F_{nfric}$	Normal force acting on friction wheel, [ $N$ ]
$F_{s1}$	Force on friction wheel motor fastener 1 , [ $N$ ]
$F_{s2}$	Force on friction wheel motor fastener 2 , [ $N$ ]
$F_{spring}$	Force applied by hinge spring, [ $N$ ]
$H_{keel}$	Height of the bearing arm contact point on the keel, [ $m$ ]

$L_G$	Width of gondola, [m]
$L_a$	Length from pivot point of hinge to fastener a , [m]
$L_b$	Length from pivot point of hinge to fastener b , [m]
$L_m$	Length from side of gondola to gondola drive motor hinge, [m]
$L_s$	Length from fastener to fastener of gondola motor to hinge, [m]
$L_{SF}$	Length to snap fit bearing, [m]
$L_{ac}$	Length from centerline of gondola to fastener a, [m]
$L_{bc}$	Length from centerline of gondola to fastener b, [m]
$L_{cm}$	Length from gondola wall to center of mass of gondola, [m]
$L_{contact}$	Length from contact to contact of bearings on keel, [m]
$L_{drive}$	Length of gondola hinge to friction wheel contact, [m]
$L_{hs}$	Distance from the pivot of the hinge to the gondola motor fastener, [m]
$L_{hw}$	Distance from the gondola motor fastener to the contact point of the friction wheel, [m]
$L_{rx}$	Friction wheel motors shaft length, [m]
$M_1$	Reaction moment on bearing arm, [Nm]
$M_R$	Connector moment reaction, [Nm]
$R$	Reaction force, [N]
$S_{compressive}$	Compressive strength of gondola material, [Pa]
$T_w$	Friction wheel motor torque, [Nm]
$T_{spring}$	Torque of hinge spring, [Nm]
$W_A$	Weight of thruster assembly arm, [N]
$W_E$	Weight of thruster enclosure, [N]
$W_T$	Weight of thruster, [N]
$W_c$	Weight of connection piece, [N]
$W_{LA}$	Weight of linear actuator, [N]

$\eta$	Safety Factor
$\mu$	Coefficient of friction
$\sigma'$	Von Mises Stress, [Pa]
$\sigma_{washer}$	Compressive force of washer, [Pa]
$\sigma_x$	Principle stress, [Pa]
$\sigma_a$	Hoop stress, [N/mm <sup>2</sup> ]
$\sigma_s$	Allowable design stress for plastic, N/mm <sup>2</sup>
$a_{airship}$	Acceleration of airship, [m/s]
$a_{gondola1}$	Acceleration of Gondola 1 , [m/s <sup>2</sup> ]
$a_{gondola2}$	Acceleration of Gondola 2 , [m/s <sup>2</sup> ]
$c$	Distance from neutral axis to stress location, [m]
$d_i$	Interference diameter, [mm]
$d_s$	Hub outer diameter, [mm]
$d_s$	Shaft diameter, [mm]
$i_a$	Allowable interference, [mm]
$m_{airship}$	Mass of airship, [kg]
$m_{gondola1}$	Mass of Gondola 1, [kg]
$m_{gondola2}$	Mass of Gondola 2, [kg]
$r_{fw}$	Radius of friction wheel, [m]
$w_{armx}$	Width of the bearing arm in the x direction, [m]
$w_{army}$	Width of the bearing arm in the y direction, [m]



# Chapter 1: Introduction

## 1.1 Project Mandate

The goal of the project is to overcome the current limitations involved with the control of unmanned airships in adverse outdoor conditions. The airship consists of a helium filled envelope, external keel, and gondola which will act as a ballast. The moving ballast will control the pitch by the controlled displacement of the centre of mass. Propulsion will be provided by propellers in the X-Y plane of the airship. The system will have vector thrusting to allow for altitude change independent of pitch change.

## 1.2 Group Problem Scope

The research project led by Dr. Eric Lanteigne involves designing a system to allow for the control of an unmanned airship. The goal of the project is to create a system that controls the airship by changing the position of the centre of mass to initiate pitch change. This pitch change, along with forward propulsion, will drive the airship in a given direction. The design team will be responsible for creating a system, where a gondola that acts as a ballast will move along a non-linear, diamond-shaped keel in order to initiate pitch change of an airship. Ideally, the system will be able to achieve a pitch change of up to ninety degrees, allowing the airship to descend straight downwards. Currently, all designs must be scalable as specifications of the airship envelope have yet to be finalized. The unmanned airship must be capable of flying outdoors in wet conditions and be able to carry a payload of between 0.2kg and 0.5kg. Landing/mooring will not be an issue, and thus is outside of the project scope, as it will be grabbed by an individual during descent.

## 1.3 Criteria and Restrictions

The propellers will be in the X-Y plane, in line with the centre of volume. This eliminates any moments from the propellers that lead to imbalance and unwanted pitch variations. The gondola will be able to move along the varying curvature of the keel using a hinged-gondola. The driving mechanism will be two friction wheels with the additional support of 4 driven bearings. The cross-section of the keel is diamond-shaped, however it is not torsionally constant, therefore the vertexes are not coincident on the curved section. Once the airship has been constructed, a Special Flight Operations Certificate (SFOC) issued by Transport Canada will be necessary in order to fly the airship lawfully.

## 1.4 Parametrization Overview

A high level overview of the system's parametrization is shown in Figure 1.1.

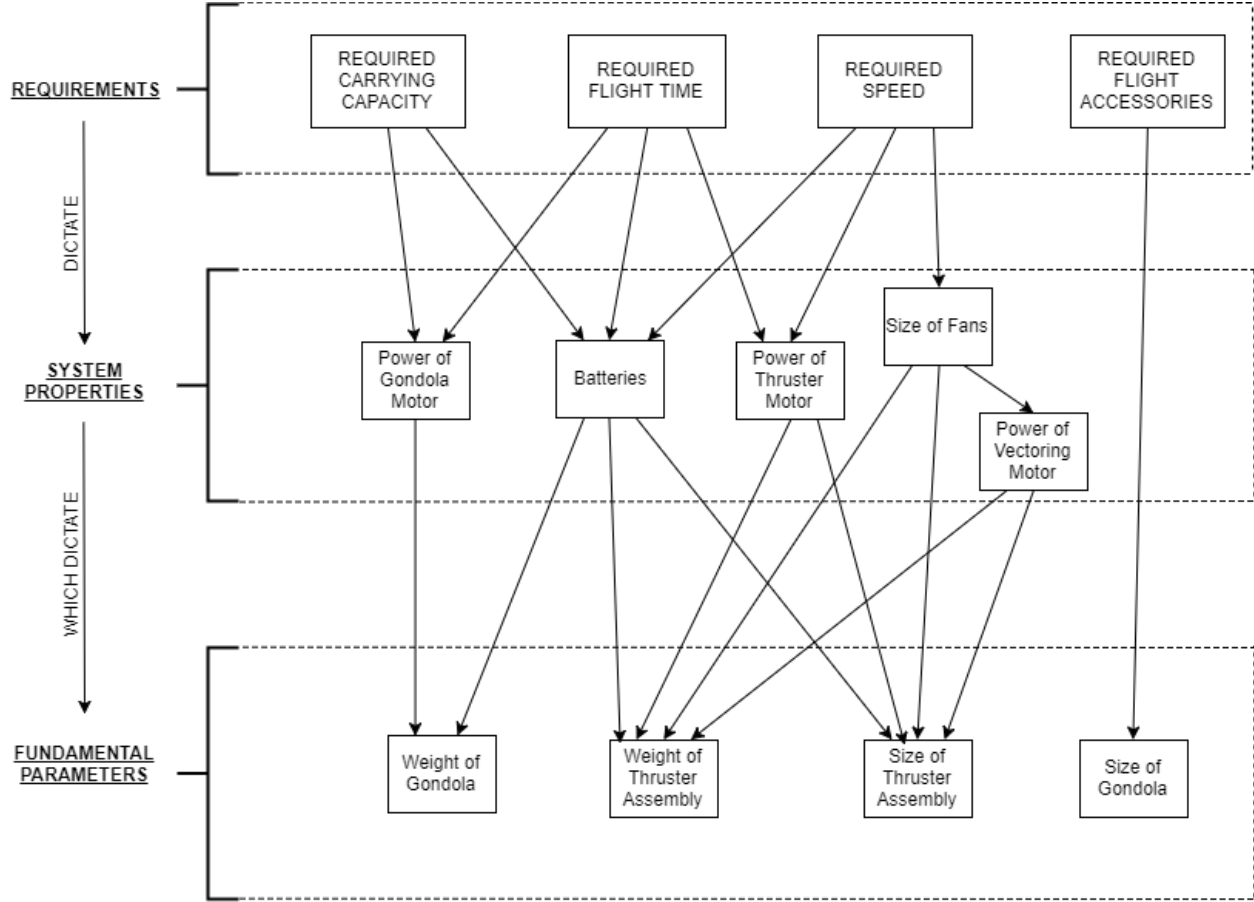


Figure 1.1: Overview of Modelling Parametrization

This outline conveys the extreme interdependencies involved in parametrizing the airship. Each input parameter impacts almost every output parameter, making total parametrization non-linear. The Parametrization outline for the entire airship can be seen in Figure ??.

# Chapter 2: Analysis

## 2.1 Outline

Table 2.1: List of All Parametrized Components

Section	Analysis	Parametrized Part	Failure Likelihood
2.3.5	Envelope Dimensions	Length of Envelope	LOW (SEE SECTION 2.3.5 )
		Diameter of Envelope	
		Radius of Envelope Support	
		Radius of Thruster Arms	
2.4.1	Thruster Assembly Component Selection	Thruster Battery (See Log File)	MEDIUM
		Propeller Diameter	
		Motor (See Log File)	
		Thruster Shaft Length	
		Diameter of Propeller Encasement	
		Component Cover Dimensions	
2.4.2	Thruster Shaft	Diameter of Thruster Shaft	HIGH
		Thread Type (See Log File)	
		Bearing Dimensions	
		Bearing Bracket Dimensions	
		Nut and Washer Dimensions	
		Propeller Motor Mounting Bracket Dimensions	
2.4.3	Thruster Arms	Thickness	HIGH
		Thickness of Arm Cap	
2.4.4	Connection To Keel	Thickness of Insert	HIGH
2.4.5	Friction Wheel Slip	Spring Torque (See Log File)	
		Motor Torque (See Log File)	
2.4.6	Gondola Hinge Bolts	Diameter of Washers	MEDIUM
2.4.7	Linear Actuator	Linear Actuator Selection (See Log File)	LOW
2.4.8	Gondola Bearing Arms	Diameter of Bearing Arms	HIGH
2.4.9	Gondola Bearing Snap-Fit	Depth of Cut	HIGH
		Bevel of Cut	

Table 2.2: List of All Inconsequential Analysis

Section	Inconsequential Analysis	Failure Likelihood
C.1	Gondola Arm Deflection	LOW
C.2	Gondola Arm Fatigue	LOW
C.3	Thruster Assembly Arm Adhesion	LOW
C.4	Gondola Motor Shaft	LOW
C.5	Axial Loading of Vectoring Shaft	LOW
C.6	Vectoring Motor Power	LOW
C.7	Gondola Motor Hinge	LOW
C.8	Bearings	LOW

## 2.2 High Level Parametrization

BIG TING HERE

## 2.3 System Modelling

### 2.3.1 Thrusters

The thruster will be balanced so that the servo motor will only use power when actively rotating the thruster. As a result, when the thruster is vectored straight forward, it will not be able to move the shaft assembly due to the inertia of the parts and the minimal resistance in the servo motor. The same effect will be present when the thruster is vectored vertically.

Given the high angular velocity and non-negligible inertia of the propeller, the system will be subject to gyroscopic forces if the thruster orientation is changed in flight. To counter the addition of unwanted high forces to the components, power to the thruster will be cut and if need be, applied in the reverse orientation for a specific duration before the thruster is reoriented. This reduction or elimination of angular velocity will effectively render gyroscopic forces negligible or eliminate them all together.

Also, the analysis done on the thruster motor did not present considerable results and can be found in Appendix section ???. The propeller will be well balanced eliminating any detrimental rotating imbalances. The motor mounting bracket will secure the motor using screws, which do not need to be analysed as the stresses applied are negligible compared to the strength of the material.

### 2.3.2 Gondola Forces

In order to complete the analysis on the gondola there are numerous forces and reaction that need to be computed. Reaction forces are solved using the gondolaForces code REF??? in conjunction with forceSolver which is explained in section REF?? and the rotate code REF???. The gondolaForces code required the inputs of all the known forces acting on the gondola and their positions including the drive force of the friction wheel motor, the spring force acting on the friction wheel, the maximum thruster acceleration, the weight of each gondola car, and the linear actuator holding force. The code also requires the pitch angle of the airship ( $\phi$ ), the thruster angle ( $\beta$ ), the angle between the gondola cars( $\Theta$ ), the position of each of the bearing arm reactions. All of the angles mentioned above are with reference to the top surface of the rear gondola. The code will output acceleration of the gondola, The maximum force applied by the bearing arms and the braking force if the linear actuator is applied.

the coordinate system in which all the forces are referenced is based on the rear gondola (gondola 1) as seen in FIG ???. The code first takes the drive force and the spring force both of which are acting on the friction wheels and rotates them into the coordinated system of the rear gondola based on the 45 degree angle of the torsion hinge. The spring and drive force acting on the front gondola (gondola 2) are again rotated based on the angle between the gondolas ( $\Theta$ ). Then the code takes the inputed maximum thrust acceleration, rotates it based on the thrust angle ( $\beta$ ) multiplies it by the mass of each gondola car and applies it to the center of mass of the corresponding gondola car. The weight of each car is then based on the pitch angle ( $\phi$ ) is then also applied to the center of mass of each gondola car. For the case where the linear actuator is applied that force is included and the braking force in the x direction is equated to the sum of all other forces acting in that direction up to the maximum capable braking. The maximum capable breaking is determined in the linear actuator analysis 2.4.7. The sum of forces in x y and z in there most general form are presented below with the reactions on the left of the equal sign and the forces on the right.

$$\begin{aligned} \Sigma F_x : (m_1 + m_2)a_{gondola} + F_{NB3_x} + F_{NB4_x} = \\ \sin(\phi)(m_1 + m_2)g + F_{Drive} + \cos(\Theta)F_{Drive} + \cos(\beta)(m_1 + m_2)a_{Thrust} + \frac{\sqrt{2}}{2}\sin(\Theta)F_{Spring} + F_{Brake} \end{aligned} \quad (2.1)$$

$$\Sigma F_y : F_{NB1_y} - F_{NB2_y} - F_{NB3_y} + F_{NB4_y} = \frac{\sqrt{2}}{2}F_{Spring} - \frac{\sqrt{2}}{2}F_{Spring} \quad (2.2)$$

$$\begin{aligned} \Sigma F_z : F_{NB1_z} + F_{NB2_z} + F_{NB3_z} + F_{NB4_z} = \\ \cos(\phi)(m_1 + m_2)g - \frac{\sqrt{2}}{2}\cos(\Theta)F_{Spring} - \frac{\sqrt{2}}{2}F_{Spring} + \sin(\beta)(m_1 + m_2)a_{Thrust} + \sin(\Theta)F_{Drive} + F_{LA} \end{aligned} \quad (2.3)$$

Force solver ??? is used to solve these equations while making some assumptions based on the reactions. All of the  $F_{NB}$  the normal forces between the bearings and the keel. since the contact surface is at 45 °between the XY and XZ planes, the magnitudes of the forces acting in the z and y directions must be equal.

$$F_{NB1_z} = -F_{NB1_y} \quad (2.4)$$

$$F_{NB2_z} = F_{NB2_y} \quad (2.5)$$

For the bearings on the front gondola as a result of the angle between gondolas, there will also be a

force acting in the x direction such that

$$F_{NB3_x} = -\tan(\Theta)F_{NB3_z} \quad (2.6)$$

$$F_{NB4_x} = -\tan(\Theta)F_{NB4_z} \quad (2.7)$$

$$F_{NB3_y} = -\frac{F_{NB3_z}}{\cos(\Theta)} \quad (2.8)$$

$$F_{NB4_y} = \frac{F_{NB4_z}}{\cos(\Theta)} \quad (2.9)$$

The above equations from 2.4 to 2.9 are all encompassed by the switch case, scenario 2, in the Force Solver Code????.

### 2.3.3 Loading Scenarios

#### Maximum Required Gondola Drive Force

The following scenario shown in FIG??? is the one that would require the greatest drive force from the gondola friction wheel motors. The assumptions made for this scenario are extremely conservative in that the scenario is extremely unlikely to actually occur but would result in considerably greater forces acting against the gondola motors than any more likely situation. The scenario involves the airship pitching straight upwards (pitch angle  $\phi$  of 90 degrees), thrusting straight upwards at full thrust (thrust angle  $\beta$  of 0 degrees) and the gondola is on the straight section of the keel (gondola angle  $\Theta$  of 0) driving up towards the curved section of the keel.

#### Maximum Gondola Bearing Arm Forces

The scenario shown in FIG??? results in the largest forces being applied to the gondola bearing arms. The scenario involves the linear actuator being applied in order to hold the position of the gondola on the straight part of the keel. The airship has a pitch angle of 0 and the thrusters is angle is 90 degrees straight up. This loading scenario results in the largest force being applied to the bearing arms.

### 2.3.4 Drag Analysis

An analysis from a report called *Technical Manual of Airship Aerodynamics* [32] was used to determine the effect of drag on the airship. The following formula was used to compute the total drag force:

$$D = C_D \rho (vol)^{2/3} v^{1.86}$$

Where  $D$  is the drag in  $lbf$ ,  $\rho$  is the density of air [ $slugs/ft^3$ ],  $vol$  is the volume of the airship envelope [ $ft^3$ ],  $v$  is the velocity of the airship [ $ft/s$ ], and  $C_D$  is the Prandtl Shape Coefficient.

The formula is converted into metric units for simplicity, using a multiplication factor:

$$D[N] = 0.847103 * (C_D) * (\rho[kg/m^3]) * (vol[m^3])^{2/3} * (v[m/s])^{1.86} \quad (2.10)$$

For this airship,  $C_D$  is estimated using Table 2.3 below.

Table 2.3: Airship Model Characteristics and Data [32] Continued

Name of model	Length, $L$	Diameter, $D$	Surface, $S$	Area maximum cross- sectional area $A$	Volume, Vol.	Prandtl shape coefficient $C_D$			Fineness ratio, $F_R = \frac{L}{D}$	Distance maximum diameter from nose	Distance CG from nose	Prismatic coefficient, $Q = \frac{Vol.}{A-L}$	Index of form efficiency $H_F = \frac{Q}{C_D}$			
						20 m. p. h.	40 m. p. h.	60 m. p. h.					20 m. p. h.	40 m. p. h.	60 m. p. h.	
<i>Elliptical series (British)</i>																
E 1	2. 371	0. 3906	Sq. ft.	Sq. ft.	Cu. ft.	0. 120	0. 1658	0. 0132	0. 0135	6. 070	P. ct. L	P. ct. L	0	5835	44. 20	43. 22
E 2	1. 743	. 3910				. 120	. 1261	. 0138	. 0128	4. 460	33. 86			6024	43. 65	47. 06
E 3	1. 568	. 3920				. 121	. 1112	. 0147	. 0120	4. 000	34. 19			5876	40. 00	45. 55
E 4	1. 384	. 3923				. 121	. 0972	. 0167	. 0139	3. 500	35. 18			5810	34. 79	41. 80
E 5	1. 178	. 3929				. 121	. 0826	. 0184	. 0147	3. 000	33. 43			5786	31. 45	39. 36
<i>Parabolic series (British)</i>																
P 1	1. 594	. 3900				. 120	. 0970	. 0168	. 0137	4. 090	49. 39			. 5094	30. 32	37. 18
P 2	1. 598	. 3903				. 120	. 1000	. 0169	. 0176	4. 070	32. 06			. 5265	31. 15	30. 00
P 3	1. 173	. 3867				. 117	. 0729	. 0226	. 0173	3. 830	50. 35			. 5293	23. 42	30. 60
P 4	1. 217	. 3870				. 118	. 0714	. 0215	. 0193	3. 140	35. 05			. 4989	23. 20	25. 85

The aircraft dimensions shown in Table 2.3 are results of testing in a wind tunnel, used to determine drag effects on real airships. They are therefore scaled down models. The goal is to select a model that has comparable dimensions to the airship to be constructed for this project.

It can be deduced from the table that the Prandtl Shape coefficient encompasses both skin and form drag. When the fineness ratio is higher, skin friction drag will have a larger effect than form drag, so when the airspeed is increased (from 20mph to 60mph),  $C_D$  will decrease. The opposite is true with small fineness ratios, where the form drag plays a larger role, therefore the  $C_D$  increases as airspeed is increased.

As a example, assuming the blimp designed has a fineness ratio of 3.5, the comparable blimp would be the Elliptical series E 4. To be conservative, the highest  $C_D$  from the E 4 is  $C_D = 0.0167$ . The calculation is shown below, for a windspeed of 20m/s:

$$D = C_D \rho (vol)^{2/3} v^{1.86} = 0.0167 * (0.00237 \text{ slugs}/\text{ft}^3) * (122.644 \text{ ft}^3)^{2/3} * (65.616 \text{ ft}/\text{s})^{1.86} = 2.342 \text{ lbf} = 10.417735 \text{ N}$$

Based on Table 2.4, the envelope contributes 35% to the drag. Therefore the total drag will be estimated as  $D_{total} = D/0.35$ . Based on this, the total drag is found to be 29.76495N. When the 35% is factored into Equation 2.10, the coefficient changes and the final formula becomes:

$$D[N] = 2.420293983 * (C_D) * (\rho[kg/m^3]) * (vol[m^3])^{2/3} * (v[m/s])^{1.86} \quad (2.11)$$

Table 2.4: Drag Contribution for Various Airship Components [32]

	<i>Percent</i>
(1) Large nonrigids with closed cars:	
(a) Envelope	45
(b) Surfaces	20
(c) Rigging and suspension cables	15
(d) Cars	15
(e) Accessories	5
(2) Small nonrigids with open cars:	
(a) Envelope	35
(b) Surfaces	25
(c) Rigging and cables	20
(d) Cars	15
(e) Accessories	5

These estimates are meant to be extremely conservative, due to the fact that the construction of the blimp will not be perfect, and any modelling situation will not be able to capture all of the imperfections in the build.

The value of  $C_D$  will change based on the fineness ratio. In the GUI of the MATLAB program, the user will input the dimensions of the airship, and the program will calculate  $C_D$  based on the fineness ratio ( $fr$ ). The GUI will only allow the user to input dimensions which result in fineness ratios of between 3.0 and 4.0. This is due to the fact that these fineness ratios most accurately reflect the shape of the pre-existing keel. The relationship is found by curve-fitting the data in Table 2.5, which were obtained from values in Table 2.3.

Table 2.5: Fineness Ratios and Corresponding  $C_D$ 

<b>Fineness Ratio <math>fr</math></b>	<b><math>C_D</math></b>
3.000	0.0184
3.500	0.0167
4.000	0.0147
4.460	0.0138
6.070	0.0132

The resulting equation for drag coefficient is found as:

$$C_D(fr) = 0.00092642 * fr^2 - 0.010134 * fr + 0.040569 \quad (2.12)$$

Equations 2.11 and 2.12 are used in conjunction to determine the drag force acting on the blimp.

### 2.3.5 Envelope Analysis

## 2.4 Component Analysis

### 2.4.1 Thruster Assembly Component Selection

### 2.4.2 Thruster Shaft

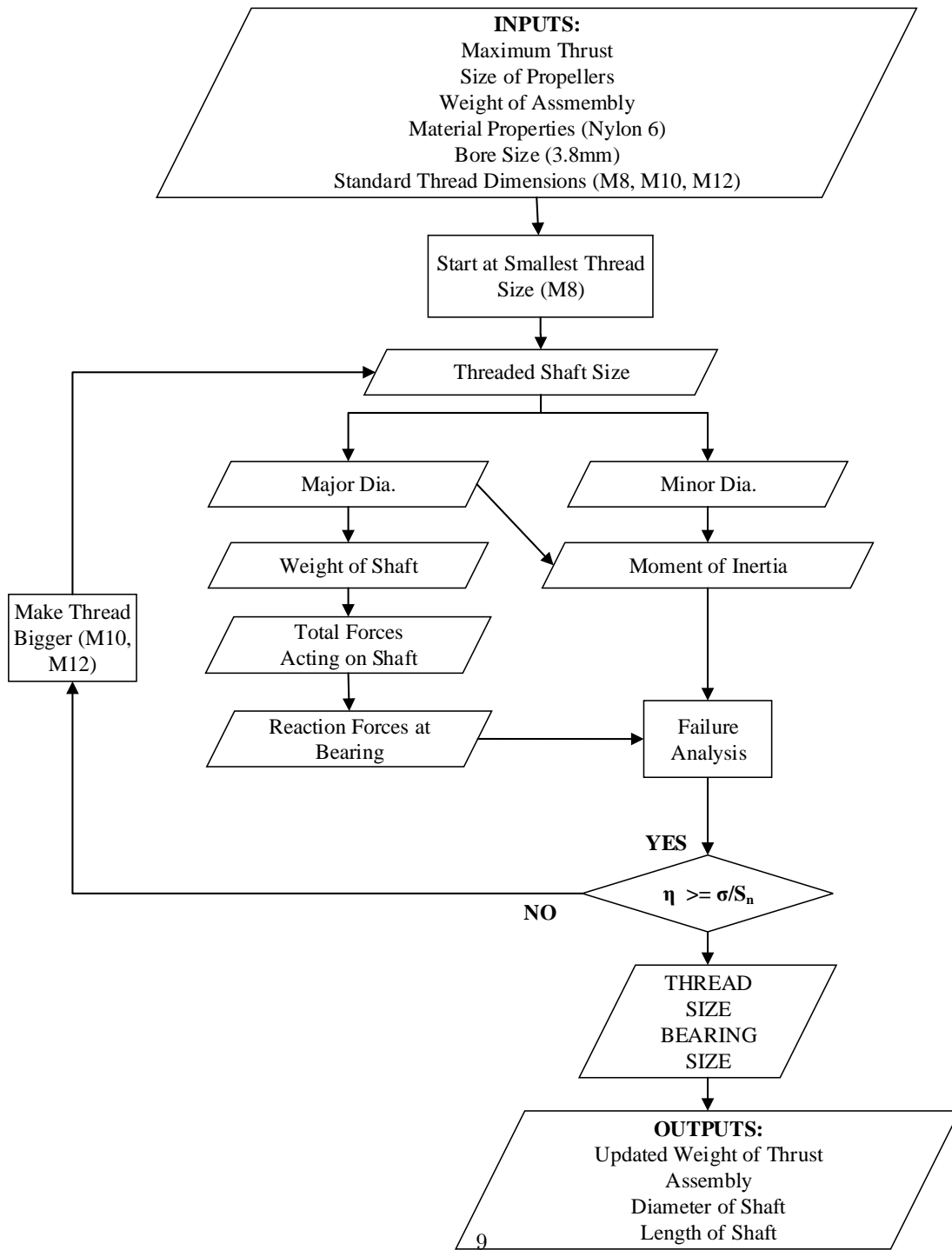


Figure 2.1: Parametrization Outline for the Thruster Shaft

The thruster shaft analysis will optimize the diameter of the thruster shaft based on standard threaded shaft dimensions. The Analysis will output the diameter of the shaft, the thread of the shaft, the length of the shaft, the weight of the shaft from which it updates the weight and centre of gravity of the entire thruster assembly. The inputs required for the analysis are the maximum thrust, the size of propellers, the weight of the assembly, the material properties of Nylon 6 REF?? (the shaft material), the bore size of the shaft which is 3.8[mm] and the standard thread dimensions from M8 to M16 REF ??.

The material nylon 6 was chosen because of its suitable strength and ease of manufacturability. Aluminium was also considered but would have resulted in an over engineered component or an unproportionally small radius. Results that justify this are shown at the end of the section REF??. The bore diameter of 3.8[mm] is based on the screw that attaches the shaft axially to the thrust vectoring motor, shown in FIG ??.

The shaft is analysed in simple bending where it is cantilevered at the bearing in the thrust vector motor assembly shown in figure ????. The analysis begins by calculating the required length of shaft for the propeller size and the length

### 2.4.3 Thruster Arms

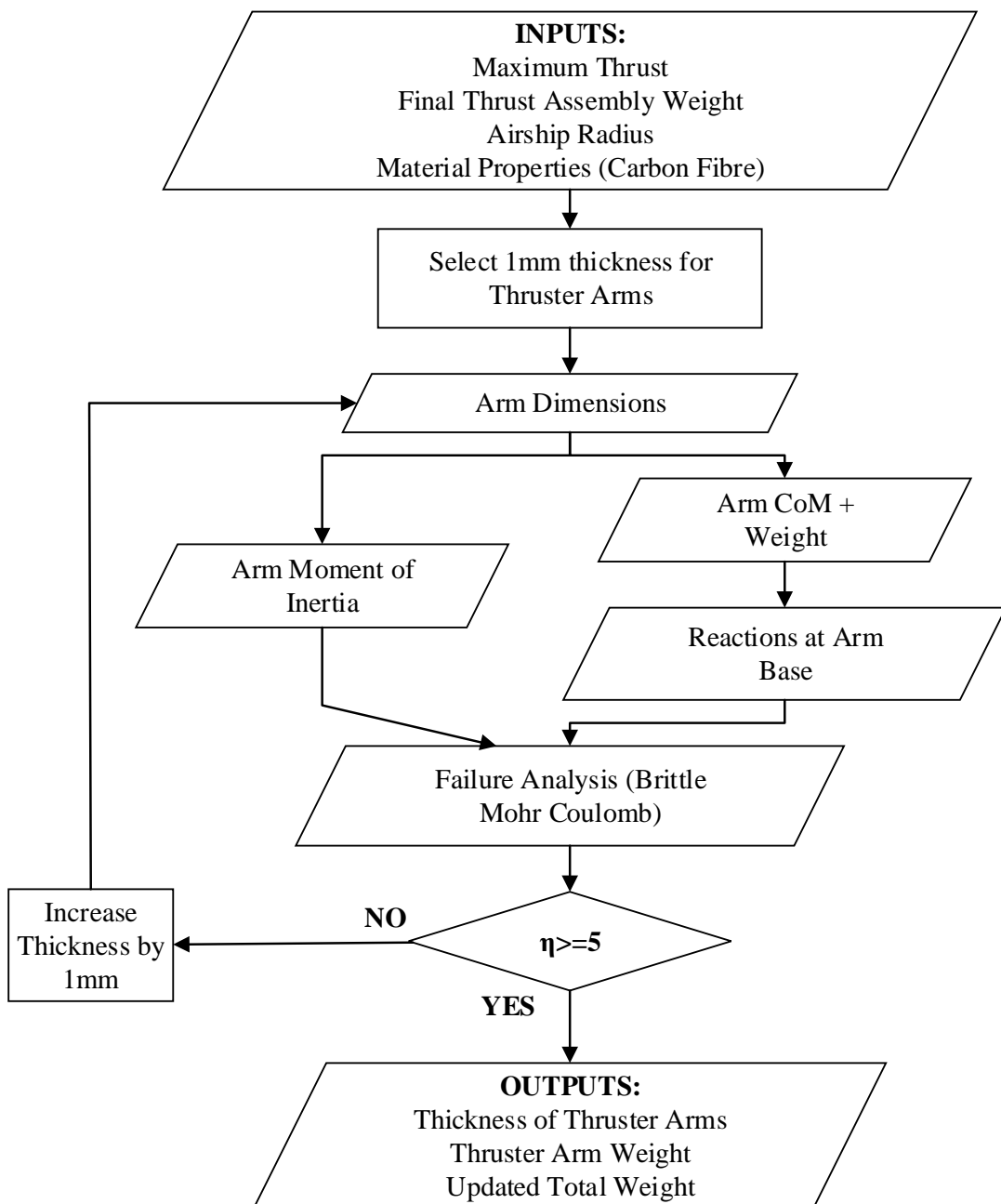


Figure 2.2: Parametrization Outline for the Thruster Arms

#### 2.4.4 Connection To Keel

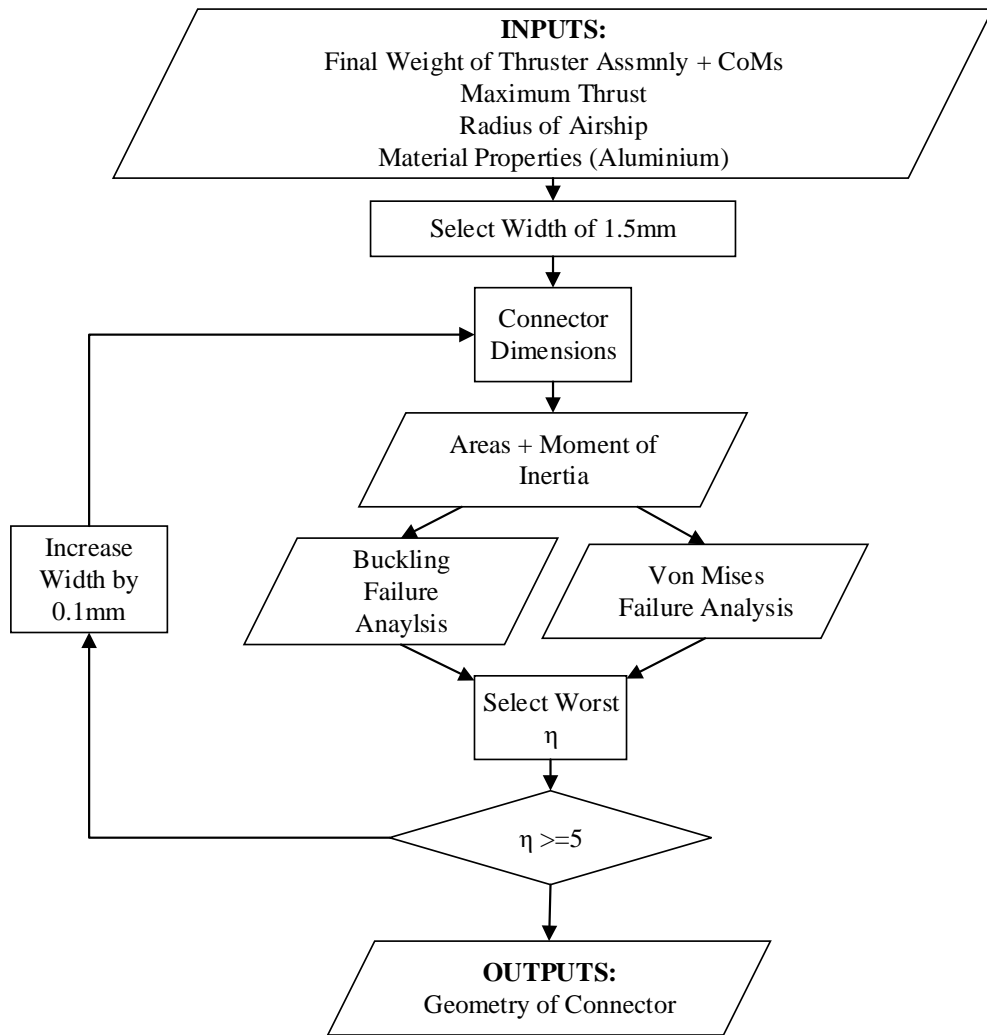


Figure 2.3: Parametrization Outline for the Thruster Arm Connector

### 2.4.5 Friction Wheel Slip

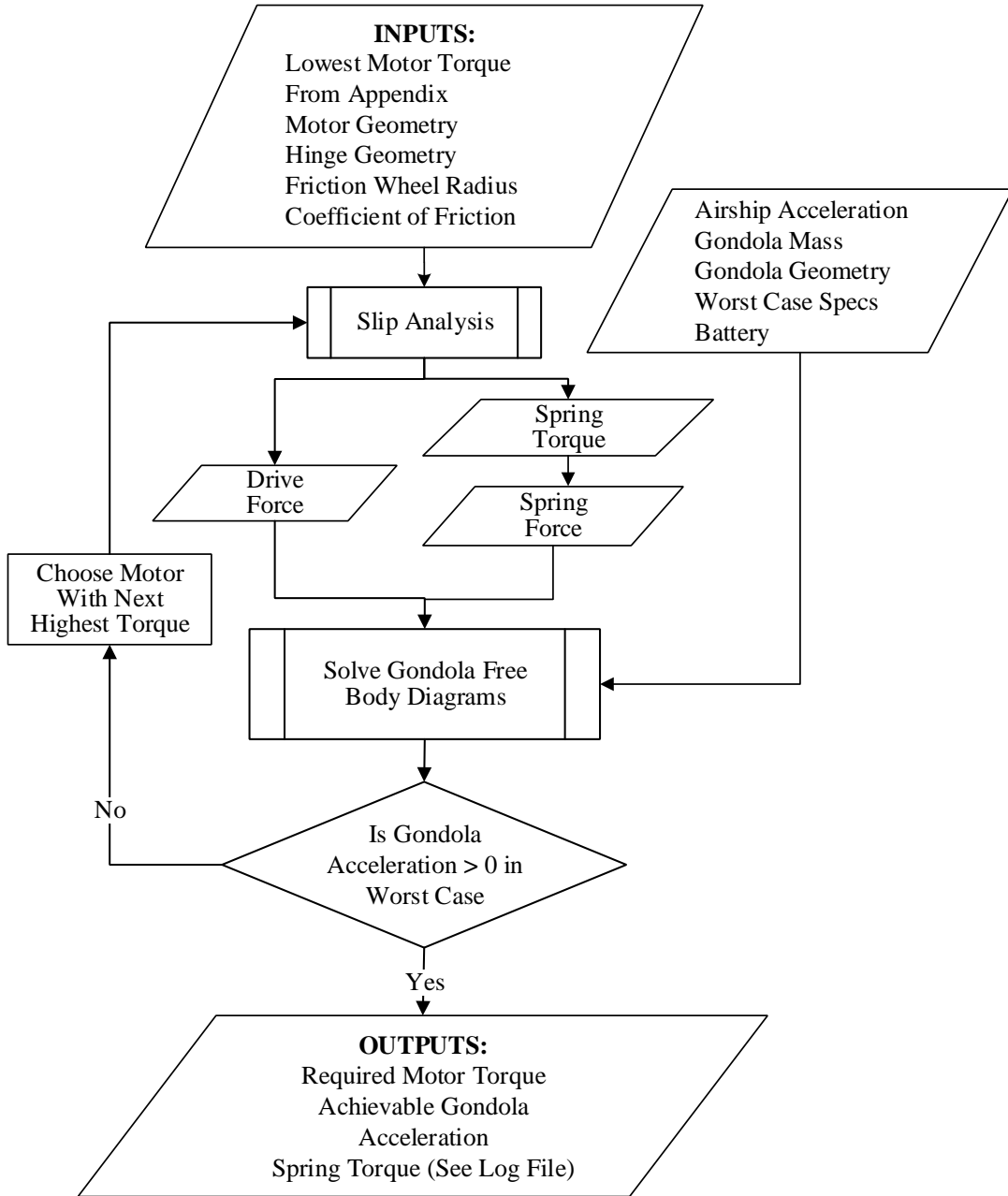


Figure 2.4: Parametrization Outline for the Friction Wheel Slip

The friction wheel slip analysis, calculates the required motor torque in order to allow for the gondola to move in a worst case scenario, and then calculates the motor hinge spring torque that will generate a large enough normal force to prevent slip of the friction wheel. The inputs required for the analysis are the geometry of the friction wheel, the motor, the hinge, the gondola, as well as the material properties of the friction wheel, the mass of each gondola car, the maximum achievable thruster acceleration and the loading

conditions specific to the worst case scenario.

The friction wheel slip analysis, calculates the required motor torque in order to allow for the gondola to move in a worst case scenario, and then calculates the motor hinge spring torque that will generate a large enough normal force to prevent slip of the friction wheel. The inputs required for the analysis are the geometry of the friction wheel, the motor, the hinge, the gondola, as well as the material properties of the friction wheel, the mass of each gondola car, the maximum achievable acceleration as a result of the thrusters and the loading conditions specific to the worst case scenario.

Parameters that will not change through out the gondola analysis include, the geometry of the motor, this is because different torques can be achieved with the same geometry by modifying the gearing. See Appendix D.4.3. The geometry of the hinge will not change as it is aluminium and the forces applied to it are minimal. The components inside of the gondola which include the R.F transmitter, the BESC and the battery will not be changing. Calculations for required power and run time are done in APPENDIX\*\*\*\*\* show that regardless of motor gearing, power requirements are easily met and the limiting factor for flight time will be the thruster batteries. As a result the geometry of the main frame of the gondola (length, width, and height) will not be parameterized and the weights of the gondola will remains approximately the same.

The analysis first assumes a motor torque. With this torque the code computes the spring torque such that  $F_{spring} = F_{Nfric}$ , which ensures the friction wheel will not slip. For the purpose of this analysis, the friction wheel and shaft interface are considered without slip, and the set screw is assumed to not fail as it will be metal interfacing with plastic.

$$F_{spring} = F_{Nfric} = \frac{F_{fFric}}{\mu} = \frac{T_w}{r_{Fw} \cdot \mu} \quad (2.13)$$

$$F_{spring} = \frac{T_{spring}}{L_{hs} + L_{sw}} \quad (2.14)$$

$$\frac{T_{spring}}{[L_{hs} + L_{sw}]} = \frac{T_w}{r_{Fw} \cdot \mu} \quad (2.15)$$

The relation for the minimum necessary spring torque is multiplied by a factor of 1.5 in order to account for any neglected external factors.

$$T_{spring} = \frac{T_w \cdot [L_{hs} + L_{sw}]}{r_{Fw} \cdot \mu} \cdot 1.5 \quad (2.16)$$

Based on the assumed torque and the spring force, the acceleration of the gondola in the worst case scenario explained in SECTION????, and FIGURE ???? The acceleration of the gondola is calculated, The forces acting The following equations 2.17 to 2.19 are the sum of forces acting on the gondola in the

coordinate system defined by the plane of the surface of the rear gondola car. As a result most of the forces and reactions acting on the front gondola need to be rotated according to the angle of the hinge,  $\Theta$  is the angle between the gondolas. Similarly  $\phi$  is the pitch angle of the airship and  $\beta$  is the angle at which the acceleration due to thrust is acting. The reactions are on the left of the equal sign and the known forces acting on the gondola are to the right of the equal sign.

$$\begin{aligned} \Sigma F_x : (m_1 + m_2)a_x + F_{NB3_x} + F_{NB4_x} = \\ \sin(\phi)(m_1 + m_2)g + F_{Drive} + \cos(\Theta)F_{Drive} + \cos(\beta)(m_1 + m_2)a_{Thrust} + \frac{\sqrt{2}}{2}\sin(\Theta)F_{Spring} \end{aligned} \quad (2.17)$$

$$\Sigma F_y : F_{NB1_y} - F_{NB2_y} - F_{NB3_y} + F_{NB4_y} = \frac{\sqrt{2}}{2}F_{Spring} - \frac{\sqrt{2}}{2}F_{Spring} \quad (2.18)$$

$$\begin{aligned} \Sigma F_z : F_{NB1_z} + F_{NB2_z} + F_{NB3_z} + F_{NB4_z} = \\ \cos(\phi)(m_1 + m_2)g - \frac{\sqrt{2}}{2}\cos(\Theta)F_{Spring} - \frac{\sqrt{2}}{2}F_{Spring} + \sin(\beta)(m_1 + m_2)a_{Thrust} + \sin(\Theta)F_{Drive} \end{aligned} \quad (2.19)$$

### 2.4.6 Bolt Compression Force

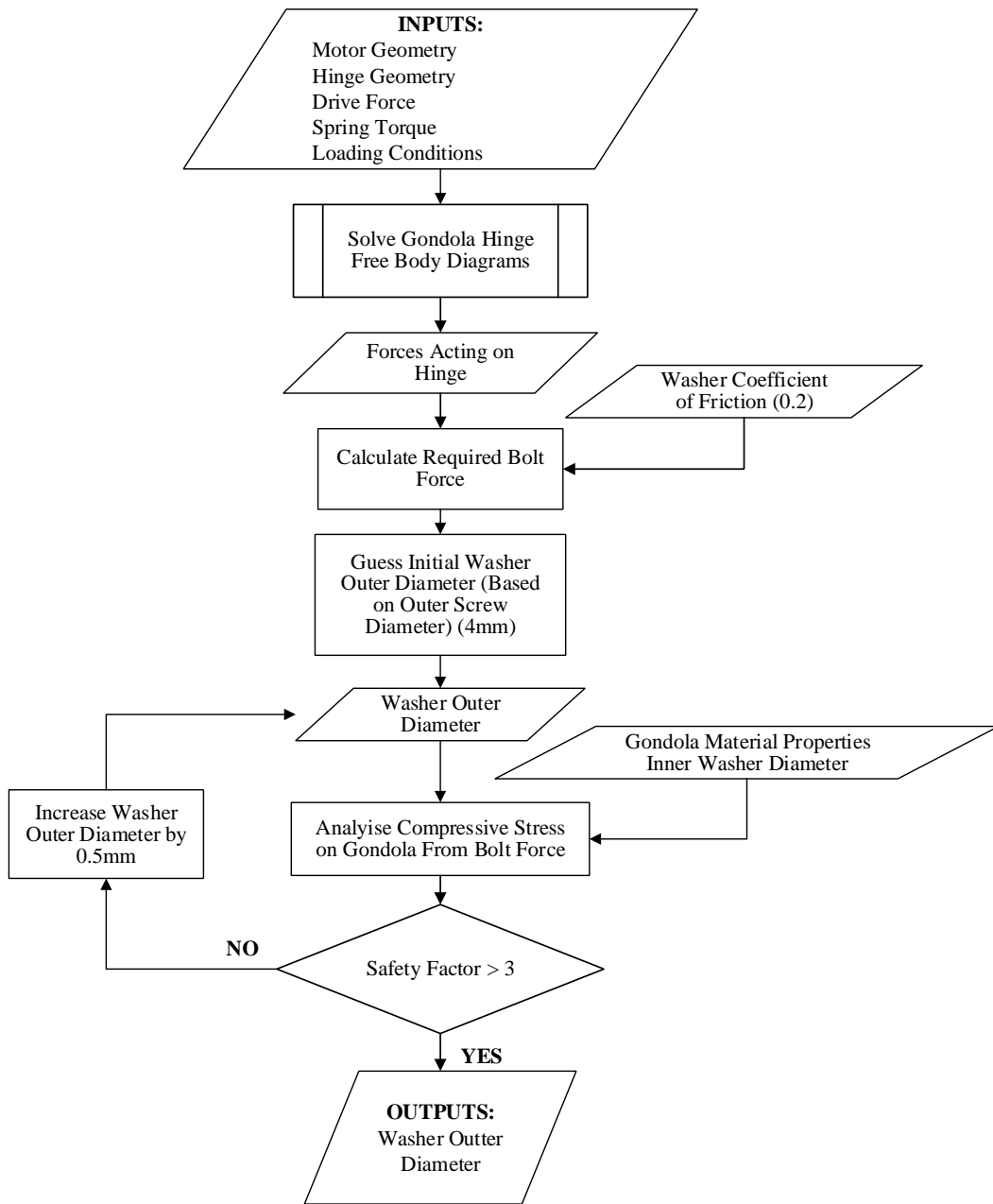


Figure 2.5: Parametrization Outline for the Bolt Compression Force

To fasten the metal hinge to the plastic gondola body, bolts will be used. The reason for this is that they use compression forces to join the two pieces, without requiring threading. Threading a screw into plastic would require female threads in 3D printed plastic, which is inherently bad design and would almost

surely fail.

The main mode of failure for the bolts will not be for the bolt itself, as the forces involved in this design will surely be much less than the yield strength of any potential bolt used. The true concern is the plastic at the interface of the bolt being crushed.

The Bolt compression analysis is meant to ensure that for the Force  $F_{bolt}$ , generated by tightening the but and bolt attaching the hinge to the gondola, that the compressive stresses are withstandable by the plastic. The required inputs for the analysis are geometry of the motor and hinge, the positions and size of the bolts used, the spring force from the hinge torsion spring and the drive force calculated from the motor torque. The analysis will output the required outer washer diameter that ensures a safety factor of 3 or greater.

The analysis first computes the bolt tension required to resist the forces parallel to the surface of the hinge. The forces parallel to the bolt are shown in Figure FREEBODY ???. The resultant forces in the XY plane are determined as

$$F_{bshear} = \sqrt{F_{bx'}^2 + F_{by}^2}$$

The only reaction resisting forces in the XY plane will be the friction between the washer and the plastic. It is known that  $F_f = \mu NormalForce$ . In this case, the normal force is provided by the bolt tension  $F_{bolt}$  shown in Figure FREEBODY ???. This bolt tensions must be large enough to generate the required friction force as well as resist the forces acting on it in the z direction. Therefore the required bolt force to ensure no slipping due to shear forces is therefore

$$F_{bolt} = \frac{\sqrt{F_{bx'}^2 + F_{by}^2}}{\mu} + F_{bz} \quad (2.20)$$

$\mu$  is estimated as the coefficient of friction between polyethylene and steel, which is 0.2 [6].

Once  $F_{bolt}$  is known, the compressive stress of the washer on the plastic gondola body can be determined. This is the critical design factor. If the compressive stress from the washer is too high it will crush the plastic underneath it.

The compressive yield strength ( $S_{compressive}$ ) of Nylon 12 is found to be 6 MPa FIND SOURCE ???. The compressive stress on the gondola by the washer is found to be

$$\sigma_{washer} = \frac{F_{bolt}}{A_{washer}}$$

$$\sigma_{washer} = \frac{F_{bolt}}{\pi(r_o - r_i)^2} \quad (2.21)$$

$$\eta = \frac{S_{compressive}}{\sigma_{washer}} \quad (2.22)$$

If the safety factor is less than 3 the analysis is reiterated with a larger washer outer radius.

### 2.4.7 Linear Actuator

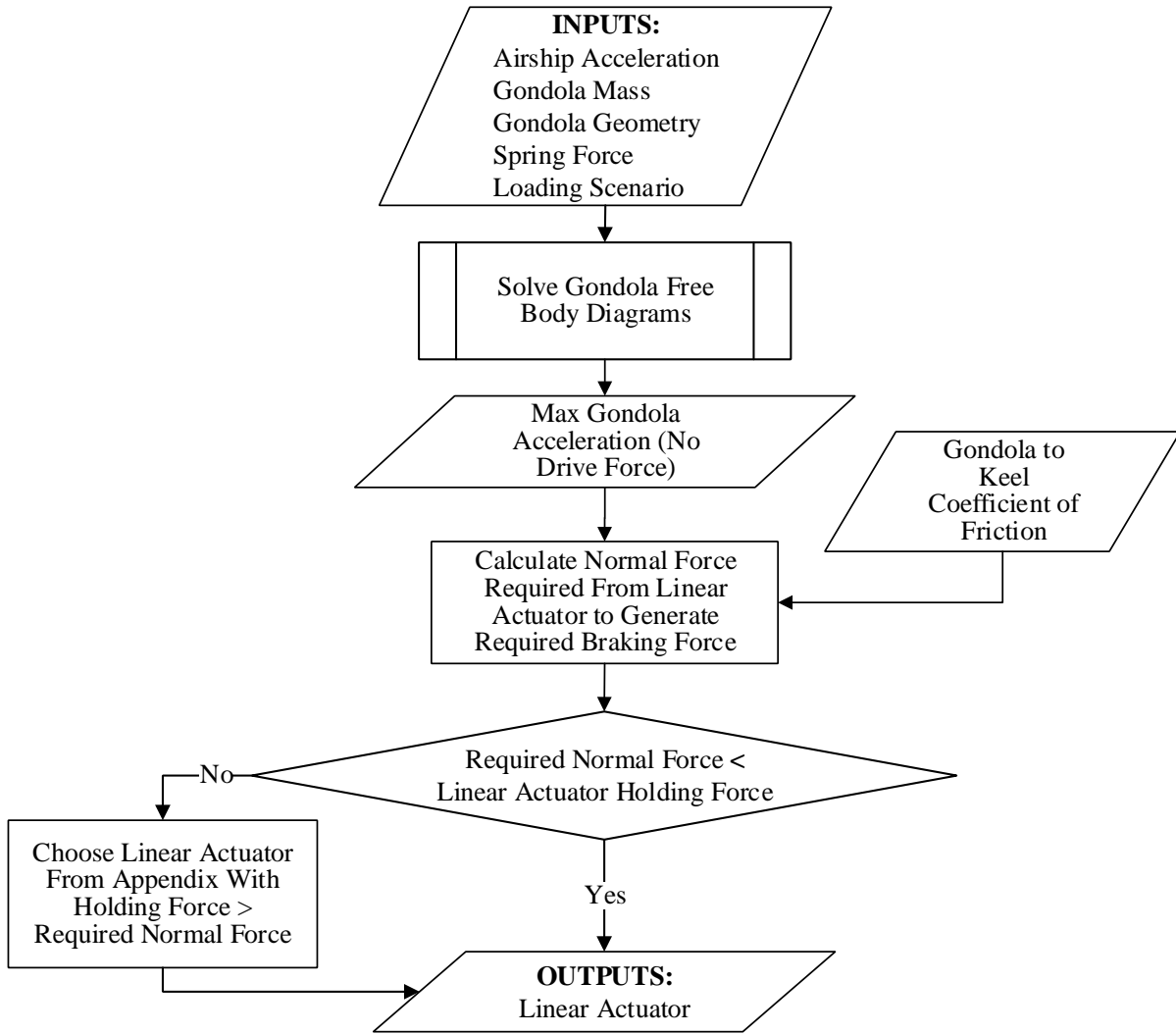


Figure 2.6: Parametrization Outline for the Bolt Compression

The linear actuator analysis is performed to ensure that the holding force of the linear actuator generates a great enough friction to keep the gondola from moving. The analysis first solves for the acceleration in a scenario similar to that of worst case mentioned above in REF???? and in friction wheel slip section 2.4.5 with the friction wheel motor not being powered, therefore the drive force  $F_{Drive} = 0$ . The inputs required to run this analysis are the geometry of the friction wheel, the motor, the hinge, the gondola, as well as the material properties of the braking surface, the mass of each gondola car, the maximum achievable thruster acceleration and the loading conditions specific to the worst case scenario. The sum of forces used

to solve for the case are as follows.

$$\begin{aligned}\Sigma F_x : (m_1 + m_2)a_x + F_{NB3_x} + F_{NB4_x} = \\ \sin(\phi)(m_1 + m_2)g + \cos(\beta)(m_1 + m_2)a_{Thrust} + \frac{\sqrt{2}}{2}\sin(\theta)F_{Spring} \quad (2.23)\end{aligned}$$

$$\Sigma F_y : F_{NB1_y} - F_{NB2_y} - F_{NB3_y} + F_{NB4_y} = \frac{\sqrt{2}}{2}F_{Spring} - \frac{\sqrt{2}}{2}F_{Spring} \quad (2.24)$$

$$\begin{aligned}\Sigma F_z : F_{NB1_z} + F_{NB2_z} + F_{NB3_z} + F_{NB4_z} = \\ \cos(\phi)(m_1 + m_2)g - \frac{\sqrt{2}}{2}\cos(\theta)F_{Spring} - \frac{\sqrt{2}}{2}F_{Spring} + \sin(\beta)(m_1 + m_2)a_{Thrust} \quad (2.25)\end{aligned}$$

The braking force  $F_{brake}$  must then be greater than the calculated acceleration  $a_x$ . The brake force is dependent on the friction force between the polyurethane and rubber contact piece of the linear actuator, as seen in Figure ???. The breaking force is related to the linear actuator for  $F_{LA}$  by the equation 2.26 below.

$$F_{brake} = \mu_{brakingsurface}F_{LA} \quad (2.26)$$

The value for  $\mu_{brakingsurface}$  is based on the coefficient of friction between rubber and polyurethane which is 0.65 CITESTION???. Once the required linear actuator force is calculated it is compared with the Actuonix linear actuator in Appendix Datasheets D.2 in order to make sure that the force is achievable.

### 2.4.8 Gondola Arm Stresses

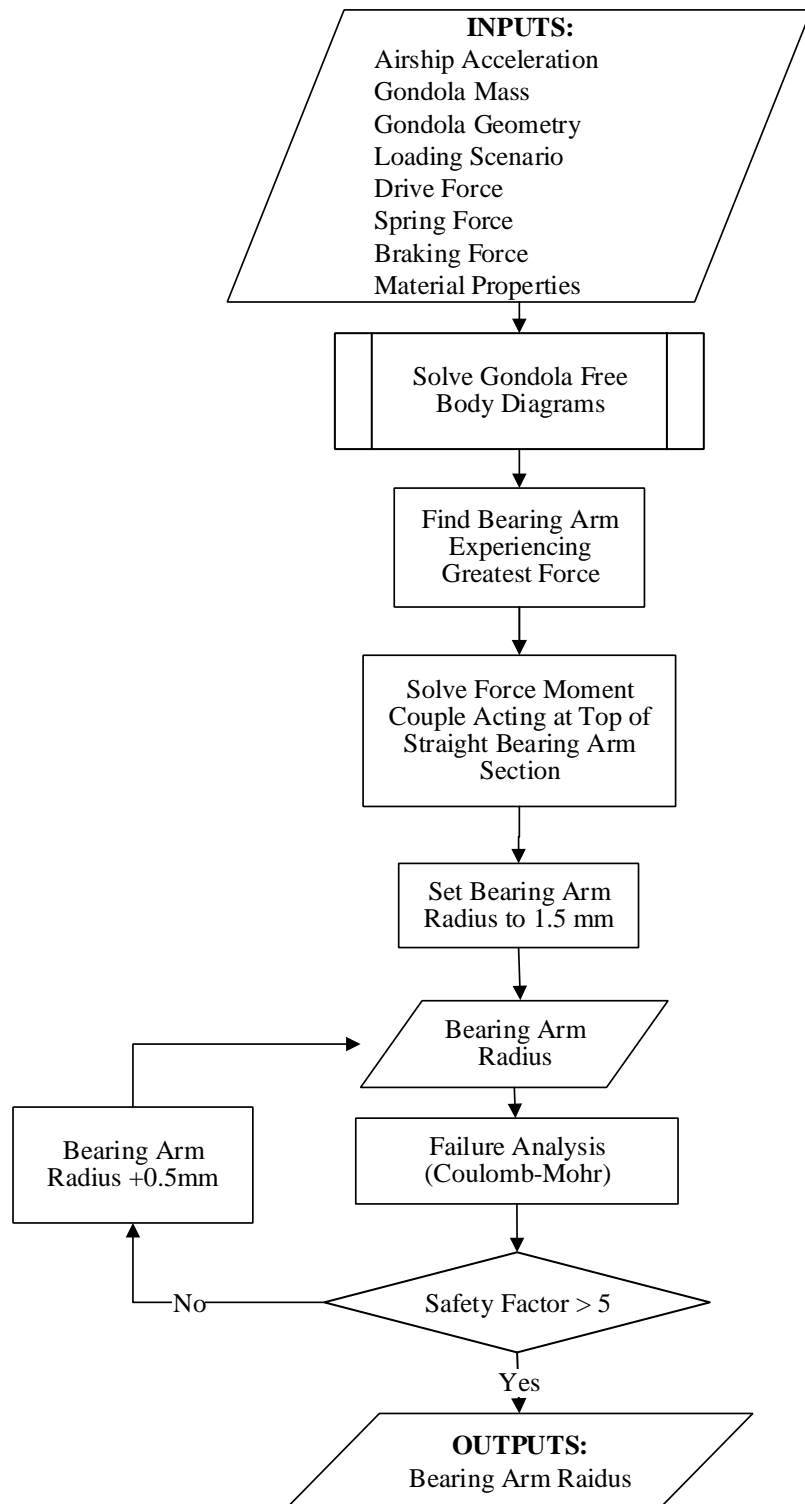


Figure 2.7: Parametrization Outline for the Gondola Arms

The failure of the gondola arm will be analysed as shown in Figure 2.8.

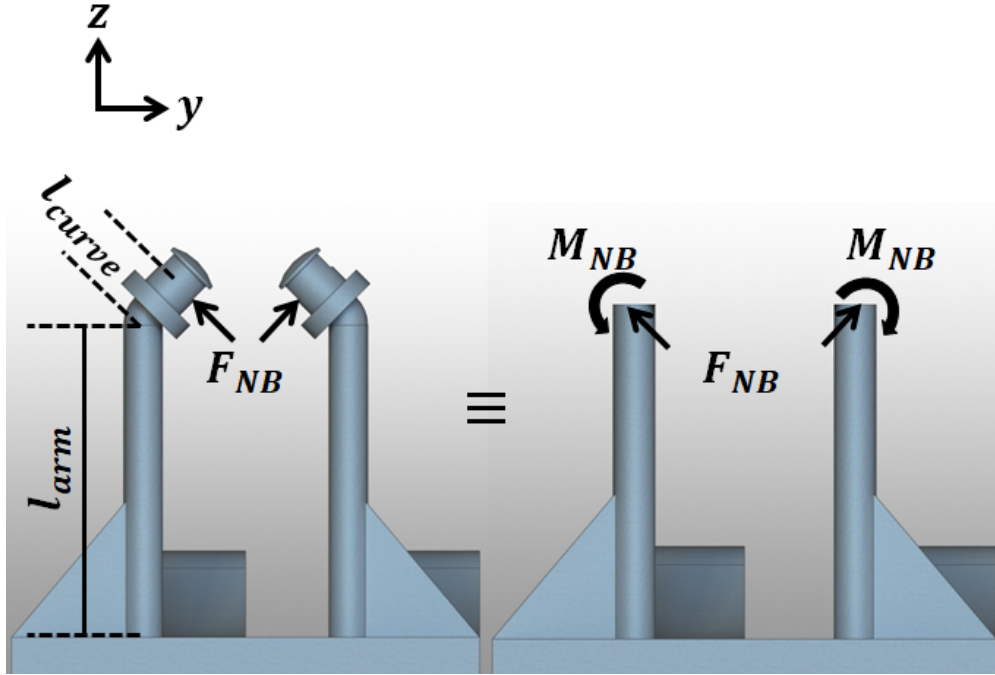


Figure 2.8: Model Used to Compute the Deflection of the Gondola Arms

For the sake of simplicity, the curved section at the very top is ignored and the force is translated from the curved section to the straight section using a force-moment couple. The moment  $M_{NB}$  is computed as  $M_{NB} = F_{NB}l_{curve}$ . Furthermore, the rib seen in Figure 2.8 is ignored. The failure criteria will be computed without the rib, and the rib will be added as an extra preventative measure, to ensure the member is rigid enough.

Three analysis were done on the gondola bearing arms. these include deflection, stress concentration analysis and fatigue analysis. However, the only analysis whose results influenced a change in design was the stress concentration. The other two can be found in Appendix sections C.1 and C.2.

The analysis first must solve the gondola forces for the case in which the greatest force is exerted on the bearing arms, when the brake is activated and the airship is thrusting upwards while the pitch remains at 0. This case is explained in REF???. The sum of forces acting on the gondola are.

$$\Sigma F_y : F_{NB1_y} - F_{NB2_y} - F_{NB3_y} + F_{NB4_y} = \frac{\sqrt{2}}{2} F_{Spring} - \frac{\sqrt{2}}{2} F_{Spring} \quad (2.27)$$

$$\begin{aligned} \Sigma F_z : F_{NB1_z} + F_{NB2_z} + F_{NB3_z} + F_{NB4_z} = \\ (m_1 + m_2)g - \frac{\sqrt{2}}{2} F_{Spring} - \frac{\sqrt{2}}{2} F_{Spring} + \sin(\beta)(m_1 + m_2)a_{Thrust} \end{aligned} \quad (2.28)$$

The sum of forces in the x direction are not shown because in this scenario, there are no forces acting in the x direction although the brake is applied. If there were any forces in the x direction since the brake is activated it would be resisted by the braking force  $F_{brake}$ . The arm that is subjected to the highest force is usually located opposite to the friction wheel, but the code REF??? will check all the bearing forces,  $F_{NB}$ , and determine which is the largest.

The member is most likely fail at the inner interface with the gondola, marked as shown in FIGURE ???. This is due to the fact that this corner will be in tension. Stress is only relevant acting upon the direction of anticipated rotation, in the x-direction. Stress at the inner corner of the arm is found as:

$$\sigma_{GondolaArm} = \sigma_{axial} + \sigma_{bendingforce} + \sigma_{bendingmoment} \quad (2.29)$$

$$\sigma_{GondolaArm} = \left( \frac{F_{NB_z}}{A} \right) \hat{k} + \left( \frac{F_{NB_y} l_{arm} c}{I} + \frac{M_{NBC}}{I} \right) \hat{j} \quad (2.30)$$

These stresses are converted to principle stresses (as shown in Appendix C.9). These principle stresses are then used to determine the safety factor by Brittle Mohr-Coulomb Theory [5, 227].

Since  $\sigma_a > \sigma_b > 0$ ,

$$\eta = \frac{S_{ut}}{\sigma_a} \Rightarrow 1.5 \geq \frac{S_{ut}}{\sigma_a} \quad (2.31)$$

### 2.4.9 Bearing Mounting (Snap-Fit)

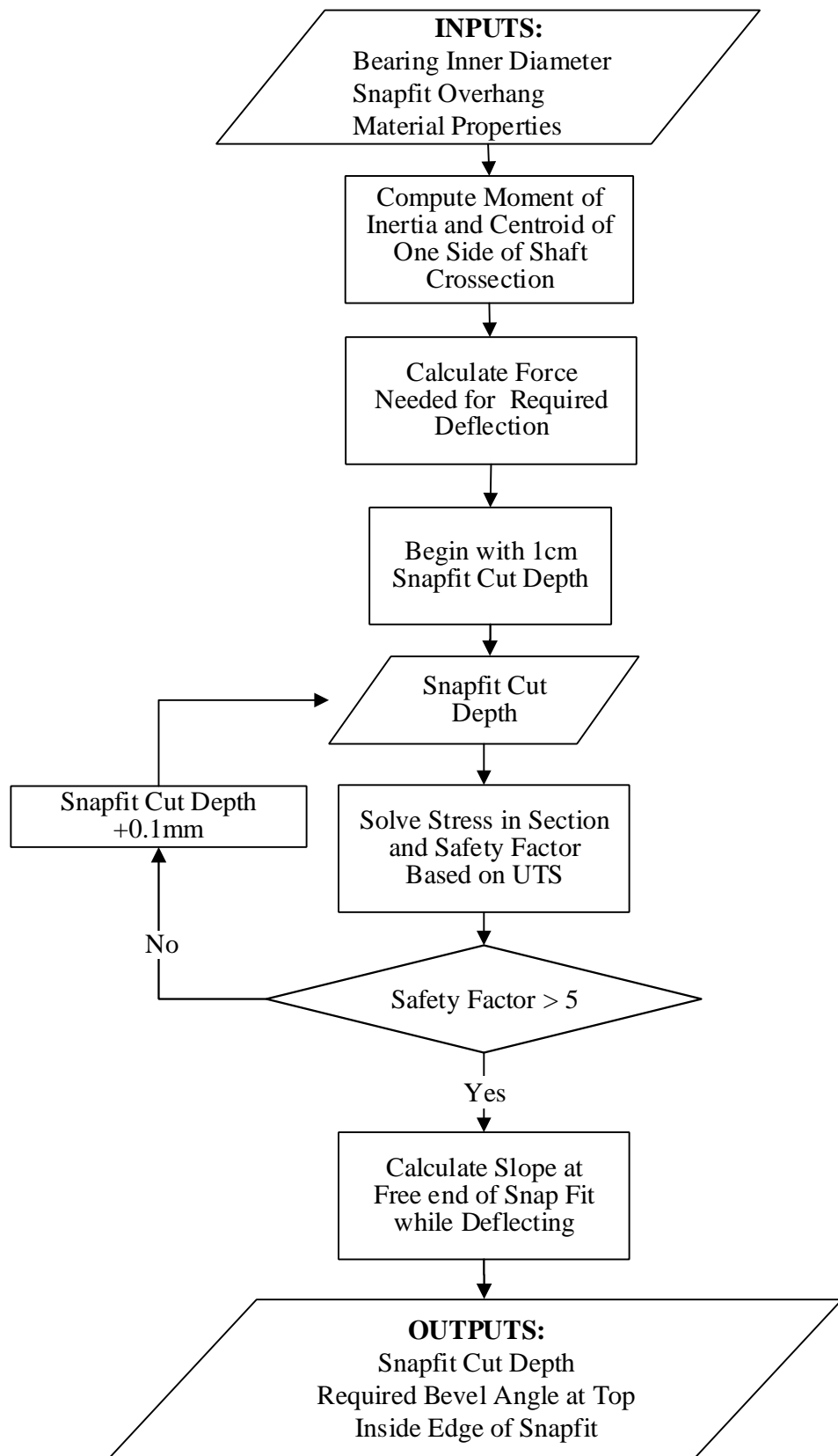


Figure 2.9: Parametrization Outline of Snapfit Analysis

The snapfit piece will be subject to a high load when the bearing is being installed, as significant deflection is necessary to allow the bearing into the grooved area. To account for this, there is a gaped section between the arms that allow for deflection. The bearing snap fit will be subject to potential failure at point at the outer edge of the shaft at the bottom of the snap fit cut shown in FIG?????. The analysis determines the minimum required cut depth in order to meet a safety factor of 1.5. The require inputs for this analysis are the bearing shaft diameter, the snap fit overhang and the material properties of nylon 12. These values are both constant as the shaft diameter is based on the inner diameter of the bearing used which will not be changing, this is justified by the analysis done in the Appendix Section ???. The choice of overhang coincides with the dimensions of the bearing used which can be seen in Appendix Datasheet D.3.

The analysis first computes the force required for the deflection that must occur for the snap fit to close to allow the bearing to slide onto the shaft. This calculation is done based on an initially chosen cut depth. The over hang is 1mm so the required deflection of each side of the snap cut is 1mm. The force required to achieve the 1mm deflection  $F_{Snapfit}$  is calculated by modeling the snap fit as a cantilever beam with a concentrated load, cantilevered at the depth of the cut into the shaft  $L_{Snapfit}$ .

$$F_{Snapfit} = \frac{3\delta EI}{L_{snapfit}^3} \quad (2.32)$$

Because of the geometry each side of the snap fit the distance the moment of inertia was calculated using the following equations REF??.  $\theta$  in the equation is the angle that forms between the point in the center of the cut edge and the outside of the cut edge as seen in Figure 2.10.

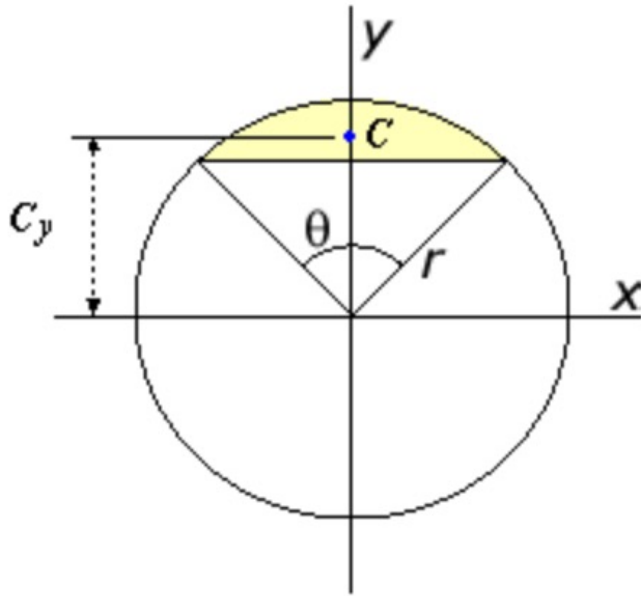


Figure 2.10: Centeroid of Section of Circle [34]

$$I = \left( \frac{r_{Snap}^4}{8} \right) \left( \theta - \sin(\theta) + 2 \sin(\theta) (\sin^2 \left( \frac{\theta}{2} \right)) \right) \quad (2.33)$$

The maximum stress  $\sigma_{Snapfit}$  will occur at the outer edge of the shaft at the bottom of the snap fit cut shown in FIG?????, and is calculated using the following equation.

$$\sigma_{Snapfit} = \frac{F_{Snapfit} L_{snapfit} c}{I} \quad (2.34)$$

The distance from the point the force is being applied to the neutral axis  $c$  in equation 2.34, is calculated by computing the length  $C_y$  from Figure 2.10 and subtracting it from the shaft radius plus the snap fit overhang. This can be seen in equation 2.35.

$$c = r_{overhang} - \frac{4r_{Snap}}{3} \left( \frac{\sin^3 \left( \frac{\theta}{2} \right)}{\theta - \sin(\theta)} \right) \quad (2.35)$$

This safety factor is slightly lower than other analysis with high failure likelihood which can be found in table 2.1. This is due to the fact that the installation will only be performed once. Maximum stress under normal loading conditions will be a direct result of the normal force applied on the bearing by the keel.

# Chapter 3: Discussion

One very large problem with the design is the fact that the component which attaches to the thruster arms and holds the thruster assembly and components is made of aluminium. This was done because the assembly which secures the thruster motor in place was a prefabricated part, chosen for simplicity for the end-user. The problem with this choice is that the bracket was metal and was to be welded to the plate for added strength. While it could have been attached by bolting or screwing, further analysis would have needed to be completed, and there was no time remaining to complete this analysis. Instead, welds were used and the assembly was over-engineered to ensure failure would not occur. In a perfect situation, the plate would be made of plastic, such as Polyethylene, and the prefabricated assembly would bolt into it. The required analysis would be completed and parts requiring parametrization would be parametrized. This change would have greatly reduced the weight of the assembly and thus helped immensely with carrying capacity.

The current model design contains many unevaluated interference fits, that are not critical design components but a safety factor has not been computed and a level of confidence has therefore not been established. Snap-fits are a suitable alternative to interference fits, although with layered 3D prints, shearing between layers is a serious concern. To improve interference fits, the temperature can be varied to create a larger interference and the materials can be changed to increase the coefficient of friction between interfaces. An interference fit was used in the gondola hinge cap, which is not ideal as any axial load in the direction of press will work against the fit. The bearing used in the thruster assembly is a standard hub fit which should not cause complications. The gondola and casing doors utilize interference, which should work although accessing components on a door while removing the door is not ideal. The propeller mounting is a standard interference fit, therefore it is not of concern. The keel connector and end stops rely on an interference fit with the keel, which means that if the keel is subject to any force in the x-direction greater than the interference fit force, the keel will become discontinuous. Likewise, if the gondola hits the end stop with too much force, the end stop will come out and the gondola will fall off the keel. The bearing snap-fit on the keel is not an ideal scenario as the direction of 3D printing will likely be at a  $45^\circ$ , meaning that half of the force is going to be shearing the plastic between the layers.

For this project, the envelope was not designed for any purpose but for reference. Dr. Lanteigne will be designing the envelope, therefore it was only design aesthetically and for the simplicity of calculating values such as volume. Given the complexity of the keel, thruster and gondola design, it would be highly beneficial to have the exact design of the envelope or to have designed it independently to have components mesh better. Variance in the envelope design have huge implications on relative performance of the airship as a whole.

---

Many components are not analysed and therefore parametrized because they are over engineered for the use. Examples of over engineered components are the bearing in the thruster assembly, the strength of fasteners, the servo mounting bracket, etc. These parts were not analysed because they are much too strong to fail in any anticipated scenarios. In retrospect, it would have been reasonable to vary the material of these components to further parametrize although conventional, off-the-shelf components will always be the least difficult to procure.

It is not reasonable to parametrize objects that vary in design between iterations, such as propeller motors. These components vary in size, shape and mounting techniques, rendering it impossible to create Solidworks models that can represent a list of different components options. The MATLAB code outputs the suggested motor and propeller options independently of the Solidworks files. This means that the some files, also including the thread on the thruster shaft are aesthetic only and the MATLAB code should be consulted for specific suggestions.

The servo motor mounting bracket is made up of several parts that are fastened using fasteners and welding techniques that create a complicated assembly procedure. This assembly is off-the-shelf with the addition of the custom bearing bracket, but the geometry required complicates the method of installation, such as the screws inside the hollow mounting block.

Generally, there are too many fasteners in this assembly, which negatively contribute to the weight limitations. Using alternatives such as welding or plastic fasteners could address this issue.

Glueing components is not the preferred method of mounting, but it is necessary in some scenarios of the design. In order to adequately mount the thruster assembly to the envelope, double sided tape will be placed along the mounting plate and onto the envelope. removing this tape will not be easy as the polyurethane could tear. Glueing the thruster arms to the thruster assembly is highly dependent on the pre-stress in the epoxy and the integrity of the weld holding the arm cap to the mounting plate. Glueing the component casing on the thruster assembly is also not an ideal scenario as it could travel while setting and it is not longer removable once place.

The friction wheel motor has a shaft size of 1mm and the friction wheel has an ID of above 6mm, therefore a shaft adapter piece is 3D printed to bridge the gap. This is not ideal as the plastic can easily be deformed and shear along the print orientation. It would be preferred if compatible sizes for the shaft and friction wheel were chosen, although this is difficult given the 1cm width of the keel. The friction coefficient used for the friction wheel and the polyurethane sheet covering the keel was estimated very roughly as there is a lack of data on the subject.

---

3D printing technology has come a long way but it is still not feasible for load bearing applications at affordable prices, therefore it is not ideal that many components are 3D printed. Material properties for 3D printed materials are only very roughly estimated and the print setting influence the properties as infill, print speed, layer height, heat, strand orientation, etc. each have a significant impact on the properties exhibited.

Carbon fibre parts are not easy to manufacture in house but given the complexity it would be difficult to commission custom moulding without the high start-up cost of mould creation (as seen in the quote obtained from an Alibaba Supplier in Appendix [? ]). Therefore the material properties of the thruster arms are highly dependent not only on the material used but also the skill of the manufacturer.

The cable glands used in the solid model are not dimensioned based on any design, they are simply assumed to be in existence. The thruster motor was not waterproofed, therefore it will likely be the weakest link when it comes to rainfall. The thruster motor can be easily removed, making this issue less critical in a potential failure.

Wiring of components was not a significant consideration. There is no consideration for how the wires will be managed within the gondolas, although this will be aesthetically pleasing as few wires are visible. A downfall of wireless communication transmission is the lack of confidence in operation overtime. The thruster shaft has a wire running through it from the components to the propeller motor, which makes wire removal difficult as well as servicing the shaft and the components attached to it.



# Bibliography

- [1] Actuonix Motion Devices. Miniature Linear Motion Series - L12, 2016. URL <https://s3.amazonaws.com/actuonix/Actuonix+L12+Datasheet.pdf>.
- [2] Advanced Mechanical Engineering Solutions. Metric Bolt Grades Strength, 2017. URL <http://www.amesweb.info/Screws/Metric\Bolt\Grades\Strength.aspx>.
- [3] Hoda Amel. *Investigating the Cyclic Performance of Laser Sintered Nylon 12*. PhD thesis, University of Sheffield, 2015. URL <http://etheses.whiterose.ac.uk/11927/1/Investigating the Cyclic Performance of Laser Sintered Nylon 12-Hoda Amel-110203386.pdf>.
- [4] Steven A. Brandt and American Institute of Aeronautics and Astronautics. *Introduction to aerodynamics : a design perspective*. American Institute of Aeronautics and Astronautics, 2004. ISBN 9781563477010.
- [5] Budynas and Nisbett. Shigley's Mechanical Engineering Design, Eighth Edition. *Analysis*, page 1059, 2006. ISSN 0717-6163. doi: 10.1007/s13398-014-0173-7.2.
- [6] Engineers Edge. Coefficients of Friction. URL <https://www.engineersedge.com/coeffients\of\friction.htm>.
- [7] Engineers Edge. Plastic Post and Hub Press Fit Equations, 2017. URL <https://www.engineersedge.com/plastic/plastic\press\fit.htm>.
- [8] Szabolcs Füzesi. Static Thrust Calculator - STRC, 2017. URL <http://www.godolloairport.hu/calc/strc\eng/index.htm>.
- [9] HobbyKing. Rhino 2250mAh 3S 11.1v 40C Lipoly Pack, . URL [https://hobbyking.com/en\us/rhino-2250mah-3s-11-1v-40c-lipoly-pack.html?{\\\_\}\{\\\_\}\{\\\_\}store=en\us](https://hobbyking.com/en\us/rhino-2250mah-3s-11-1v-40c-lipoly-pack.html?{\_\}\{\_\}\{\_\}store=en\us).
- [10] HobbyKing. TURNIGY Plush 10amp Speed Controller w/BEC, . URL <https://hobbyking.com/en\us/turnigy-plush-10amp-9gram-speed-controller.html>.
- [11] HobbyKing. Turnigy 20A BRUSHED ESC, . URL [https://hobbyking.com/en\us/turnigy-20a-brushed-esc.html?{\\\_\}\{\\\_\}\{\\\_\}store=en\us](https://hobbyking.com/en\us/turnigy-20a-brushed-esc.html?{\_\}\{\_\}\{\_\}store=en\us).
- [12] HobbyKing. PixFalcon Micro PX4 Autopilot, . URL <https://hobbyking.com/en\us/pixfalcon-micro-px4-autopilot.html>.
- [13] HobbyKing. UBLOX Micro M8N GPS Compass Module (1pc), . URL <https://hobbyking.com/en\us/ublox-micro-m8n-gps-compass-module-1pc.html>.
- [14] HobbyKing. Aerostar Carbon Fibre Propeller 7x5, . URL [https://hobbyking.com/en\us/aerostar-carbon-fibre-propeller-7x5-1pcs.html?{\\\_\}\{\\\_\}\{\\\_\}store=en\us](https://hobbyking.com/en\us/aerostar-carbon-fibre-propeller-7x5-1pcs.html?{\_\}\{\_\}\{\_\}store=en\us).

- [15] HobbyKing. FrSky TFR6M 2.4Ghz 6CH Micro Receiver FASST Compatible, . URL [https://hobbyking.com/en{\\\_}us/frsky-tfr6m-2-4ghz-6ch-micro-receiver-fasst-compatible.html](https://hobbyking.com/en{\_}us/frsky-tfr6m-2-4ghz-6ch-micro-receiver-fasst-compatible.html).
- [16] HobbyKing. HobbyKing® TM 2612 Brushless Outrunner 1900KV, . URL [https://hobbyking.com/en{\\\_}us/hobbykingr-tm-2612-brushless-outrunner-1900kv.html?gclid=CjwKCAjwgvf0BRB7EiwAeP7ehmx-1gQwKEcajtpPc1NNf0p82N1T2DdM6I-PF0INiIxTERGAn2ZBdhoCJIQQAvD{\\\_}BwE{\&}gclsrc=aw.ds](https://hobbyking.com/en{\_}us/hobbykingr-tm-2612-brushless-outrunner-1900kv.html?gclid=CjwKCAjwgvf0BRB7EiwAeP7ehmx-1gQwKEcajtpPc1NNf0p82N1T2DdM6I-PF0INiIxTERGAn2ZBdhoCJIQQAvD{\_}BwE{\&}gclsrc=aw.ds).
- [17] HobbyKing. Micro HKPilot Telemetry radio Set With Integrated PCB Antenna 915Mhz, . URL [https://hobbyking.com/en{\\\_}us/micro-hkpilot-telemetry-radio-set-with-integrated-pcb-antenna-915mhz.html](https://hobbyking.com/en{\_}us/micro-hkpilot-telemetry-radio-set-with-integrated-pcb-antenna-915mhz.html).
- [18] Lapp Group. SKINTOP ST-M Data Sheet, 2017. URL [https://products.lappgroup.com/fileadmin/documents/technische{\\\_}doku/datenblaetter/skintop/DB53111000EN.pdf](https://products.lappgroup.com/fileadmin/documents/technische{\_}doku/datenblaetter/skintop/DB53111000EN.pdf).
- [19] MatWeb. Overview of materials for Epoxy/Carbon Fiber Composite, 2017. URL <http://www.matweb.com/search/DataSheet.aspx?MatGUID=39e40851fc164b6c9bda29d798bf3726{\&}ckck=1>.
- [20] McMaster-Carr. McMaster-Carr - Neoprene Roller, Drive, Aluminum Hub, 5/8" Roller Diameter, 3/16" Roller Width, . URL <https://www.mcmaster.com/{\#}60885k31/=19r8ni4>.
- [21] McMaster-Carr. McMaster-Carr - General Purpose Plastic Ball Bearing, with Stainless Steel Ball, for 1/4" Shaft Diameter, 5/8" OD, . URL <https://www.mcmaster.com/{\#}6455k2/=19n14h4>.
- [22] McMaster-Carr. McMaster-Carr - Alloy Steel Cup-Point Set Screw, Black Oxide, 8-32 Thread, 1/4" Long, . URL <https://www.mcmaster.com/{\#}91375a190/=19r8q0o>.
- [23] McMaster-Carr. McMaster-Carr - Music-Wire Steel Torsion Spring, 180 Degree Right-Hand Wound, 0.767" OD, . URL <https://www.mcmaster.com/{\#}9271k271/=19r8qyv>.
- [24] Michigan Technological University. Properties of Selected Matrices, 2017. URL <http://www.mse.mtu.edu/{\sim}drjohn/my4150/props.html>.
- [25] Pololu. 50:1 Micro Metal Gearmotor HP 6V, . URL <https://www.pololu.com/product/998/specs>.
- [26] Pololu. Magnetic Encoder Pair Kit for Micro Metal Gearmotors, 12 CPR, 2.7-18V (HPCB compatible), . URL <https://www.pololu.com/product/3081/pictures>.
- [27] RobotShop. HS-7950TH Ultra Torque HV Coreless Titanium Gear Servo - RobotShop. URL [http://www.robotshop.com/ca/en/hs-7950th-ultra-torque-coreless-titanium-gear-servo.html?gclid=CjwKCAjwgvf0BRB7EiwAeP7ehmVw7Ku4Ih2HYJeFV34wtpf0lmQIOCX5BXYQ00f48oI4lGOzHuABnRoCKiEQAvD{\\\_}BwE](http://www.robotshop.com/ca/en/hs-7950th-ultra-torque-coreless-titanium-gear-servo.html?gclid=CjwKCAjwgvf0BRB7EiwAeP7ehmVw7Ku4Ih2HYJeFV34wtpf0lmQIOCX5BXYQ00f48oI4lGOzHuABnRoCKiEQAvD{\_}BwE).

- [28] Servo City. HS-7950TH Servo, 2017. URL <https://www.servocity.com/hs-7950th-servo>.
- [29] Gabriel Staples. Propeller Static & Dynamic Thrust Calculation - Part 1 of 2, 2013. URL <http://www.electricrcaircraftguy.com/2013/09/propeller-static-dynamic-thrust-equation.html>.
- [30] Gabriel Staples. Propeller Static & Dynamic Thrust Calculation - Part 2 of 2, 2015. URL <http://www.electricrcaircraftguy.com/2014/04/propeller-static-dynamic-thrust-equation-background.html>.
- [31] The 3D Printed Solutions Company. FDM Nylon 12, 2017. URL [http://global72.stratasys.com/~/media/Main/Files/Materials/SpecSheets/MSS\\_FDMNylon0317aWeb.pdf](http://global72.stratasys.com/~/media/Main/Files/Materials/SpecSheets/MSS_FDMNylon0317aWeb.pdf).
- [32] War Department. Technical Manual of Airship Aerodynamics. Technical report, Washington, 1941. URL [https://www.faa.gov/regulations/policies/handbooks/manuals/aviation/media/airship\\_aerodynamics.pdf](https://www.faa.gov/regulations/policies/handbooks/manuals/aviation/media/airship_aerodynamics.pdf).
- [33] Wikipedia. Cauchy Stress Tensor, 2017. URL [https://en.wikipedia.org/wiki/Cauchy\\_stress\\_tensor](https://en.wikipedia.org/wiki/Cauchy_stress_tensor).
- [34] Wolfram. Engineering Fundamentals: CENTROID, AREA, MOMENTS OF INERTIA, POLAR MOMENTS OF INERTIA, & RADIUS OF GYRATION OF A CIRCLE. URL <http://www.efunda.com/math/areas/CircularSegment.cfm>.



# Appendix A: Instructions for Installing and Running the GUI

yep



# Appendix B: Code

## B.1 Code 1

```
1 function lab1
2
3 disp('_____');
4 disp('_____');
5 disp('| Lab 1 |');
6 disp('_____');
7 disp('_____');
8
9
10 % Point we are using as x_i
11 x = 5.0;
12
13 % Delta x's that we will use in our finite-difference approximations
14 dx1 = 0.5;
15 dx2 = dx1/2;
16 dx3 = dx2/2;
17 dx4 = dx3/2;
18 dx5 = dx4/2;
19
20 % Exact derivative of y at x=5
21 exact1 = dy(5.0);
22
23 %%%%%%
24 % Approximation of the first derivative
25
26 approx11 = dyapprox(x, dx1);
27 approx12 = dyapprox(x, dx2);
28 approx13 = dyapprox(x, dx3);
29 approx14 = dyapprox(x, dx4);
30 approx15 = dyapprox(x, dx5);
31
32 % Errors using first-order method
33 disp('Errors for first-order finite-difference , (first column of table)')
34 error11 = abs(exact1 - approx11)
35 error12 = abs(exact1 - approx12)
36 error13 = abs(exact1 - approx13)
37 error14 = abs(exact1 - approx14)
38 error15 = abs(exact1 - approx15)
```

```

40 % Order of convergence
41 disp('Actual order of convergence for first-order method, (second column of table)')
42 order11 = log(error12/error11)/log(dx2/dx1)
43 order12 = log(error13/error12)/log(dx3/dx2)
44 order13 = log(error14/error13)/log(dx4/dx3)
45 order14 = log(error15/error14)/log(dx5/dx4)
46
47%%%%%%%%%%%%%
48 % Approximation of the second derivative
49
50 %Exact second derivative of y at x=5
51 exact2 = d2y(5.0);
52
53 approx21 = d2yapprox(x, dx1);
54 approx22 = d2yapprox(x, dx2);
55 approx23 = d2yapprox(x, dx3);
56 approx24 = d2yapprox(x, dx4);
57 approx25 = d2yapprox(x, dx5);
58
59 % Errors using first-order method
60 disp('Errors for first-order finite-difference, (first column of table)')
61 error21 = abs(exact2 -approx21)
62 error22 = abs(exact2 -approx22)
63 error23 = abs(exact2 -approx23)
64 error24 = abs(exact2 -approx24)
65 error25 = abs(exact2 -approx25)
66
67 % Order of convergence
68 disp('Actual order of convergence for first-order method, (second column of table)')
69 order21 = log(error22/error21)/log(dx2/dx1)
70 order22 = log(error23/error22)/log(dx3/dx2)
71 order23 = log(error24/error23)/log(dx4/dx3)
72 order24 = log(error25/error24)/log(dx5/dx4)
73
74%%%%%%%%%%%%%
75 % Approximation of the third derivative
76
77 %Exact third derivative of y at x=5
78 exact3 = d3y(5.0);
79
80 approx31 = d3yapprox(x, dx1);
81 approx32 = d3yapprox(x, dx2);
82 approx33 = d3yapprox(x, dx3);
83 approx34 = d3yapprox(x, dx4);
84 approx35 = d3yapprox(x, dx5);

```

```

85
86 % Errors using first-order method
87 disp('Errors for first-order finite-difference, (first column of table)')
88 error31 = abs(exact3 -approx31)
89 error32 = abs(exact3 -approx32)
90 error33 = abs(exact3 -approx33)
91 error34 = abs(exact3 -approx34)
92 error35 = abs(exact3 -approx35)
93
94 % Order of convergence
95 disp('Actual order of convergence for first-order method, (second column of table)')
96 order31 = log(error32/error31)/log(dx2/dx1)
97 order32 = log(error33/error32)/log(dx3/dx2)
98 order33 = log(error34/error33)/log(dx4/dx3)
99 order34 = log(error35/error34)/log(dx5/dx4)
100
101%%%%%%%%%%%%%
102%%%%%%%%%%%%%
103% Produce plots
104%%%%%%%%%%%%%
105%%%%%%%%%%%%%
106
107% Number of points in the plots
108% - Adjust this to adjust how small Delta x gets.
109% It starts at 1/2 and is divided by 2 "n" times
110 n = 33;
111
112% Initialize Storage
113 dxs = zeros(n,1);
114 errors1 = zeros(n,1);
115 errors2 = zeros(n,1);
116 errors3 = zeros(n,1);
117
118% loop through, filling "d_xs", "errors1", "errors2", and "errors3".
119 for i = 1:n
120 % Each time through the loop, Delta x is half as big
121 d_xs(i) = 0.5^i;
122 errors1(i)=abs(exact1-dyapprox(x,d_xs(i)));
123 errors2(i)=abs(exact2-d2yapprox(x,d_xs(i)));
124 errors3(i)=abs(exact3-d3yapprox(x,d_xs(i)));
125 end
126
127% Compute the log of the inverse of delta x
128 loginvdxs = log10(1./d_xs);
129

```

```

130 % Compute the log of the errors
131 logerrors1 = log10(errors1);
132 logerrors2 = log10(errors2);
133 logerrors3 = log10(errors3);
134
135 % Compute reference lines with the expected slope
136 % - the "-2" is just an offset so that the reference
137 % line does not intersect the error line.
138 reffline1 = -3*loginvdxs -2;
139 reffline2 = -2*loginvdxs -2;
140 reffline3 = -1*loginvdxs -2;
141
142 %%%%%%
143 % Make three figures
144 figure(1);
145 plot(loginvdxs,logerrors1,'-o',loginvdxs,reffline1)
146 legend('finite-difference','reference', 'slope = -3')
147 title('Third-order finite-difference error for the first derivative as a function of Delta x')
148 xlabel('log10(1/Delta x)')
149 ylabel('log10(error)')
150
151 figure(2);
152 plot(loginvdxs,logerrors2,'-o',loginvdxs,reffline2)
153 legend('finite-difference','reference', 'slope = -2')
154 title('Second-order finite-difference error for the second derivative as a function of Delta x')
155 xlabel('log10(1/Delta x)')
156 ylabel('log10(error)')
157
158 figure(3);
159 plot(loginvdxs,logerrors3,'-o',loginvdxs,reffline3)
160 legend('finite-difference','reference', 'slope = -1')
161 title('First-order finite-difference error for the third derivative as a function of Delta x')
162 xlabel('log10(1/Delta x)')
163 ylabel('log10(error)')
164
165 end
166
167
168 %%%%%%
169 % The function we are analysing evaluated at x
170 %%%%%%
171 function output = y(x)

```

```

172     output = (x^3)*sin(x);
173 end
174
175 %%%%%%
176 % The exact derivative of the function we are analysing
177 % evaluated at x.
178 %%%%%%
179 function output = dy(x)
180     output = 3*x^2*sin(x)+x^3*cos(x);
181 end
182
183 %%%%%%
184 % The exact second derivative of the function we are analysing
185 % evaluated at x.
186 %%%%%%
187 function output = d2y(x)
188     output = 6*x^2*cos(x)+(6*x-x^3)*sin(x);
189 end
190
191 %%%%%%
192 % The exact third derivative of the function we are analysing
193 % evaluated at x.
194 %%%%%%
195 function output = d3y(x)
196     output = (18*x-x^3)*cos(x)+(6-9*x^2)*sin(x);
197 end
198
199 %%%%%%
200 % A third-order approximation to the derivative of y
201 % at x using a step size of "dx"
202 %%%%%%
203 function output = dyapprox(x,dx)
204     output = (1.0/(6*dx))*(-11*y(x)+18*y(x+dx)-9*y(x+2*dx)+2*y(x+3*dx));
205 end
206
207 %%%%%%
208 % A second-order approximation to the second derivative of y
209 % at x using a step size of "dx"
210 %%%%%%
211 function output = d2yapprox(x,dx)
212     output = 1.0/(dx*dx)*(2*y(x)-5*y(x+dx)+4*y(x+2*dx)-y(x+3*dx));
213 end
214
215 %%%%%%
216 % A first-order approximation to the third derivative of y

```

```
217 % at x using a step size of "dx"
218 %%%
219 function output = d3yapprox(x,dx)
220     output = 1.0/(dx*dx*dx)*(-1*y(x)+3*y(x+dx)-3*y(x+2*dx)+y(x+3*dx));
221 end
```

# Appendix C: Additional Material

## C.1 Gondola Arm Deflection

To ensure that the gondola will not fall off of the keel during operation, a deflection calculation is computed on the gondola arm. The maximum deflection of the gondola arm is modelled in a similar fashion to the Gondola Arm Stress Analysis in Section 2.4.8.

The deflection will be calculated using simple beam equations. The force  $F_{NB}$  is resolved into  $y$  and  $z$  components. The deflection is then computed in three separate parts, as shown below:

$$\delta_{GondolaArm} = \delta_{axial} + \delta_{bendingforce} + \delta_{bendingmoment} \quad (\text{C.1})$$

$$\delta_{GondolaArm} = \left( \frac{F_{NB_z} l_{arm}}{AE} \right) \hat{k} + \left( \frac{F_{NB_y} l_{arm}^3}{3EI} + \frac{M_{NB} l_{arm}^2}{2EI} \right) \hat{j} \quad (\text{C.2})$$

The failure possibility here would be for the arm to deflect enough that the gondola falls off the keel. This occurs when the total deflection  $\delta$  is larger than 0.5cm, which is half of the width of the keel face. Since both arms can deflect at the same time, they can be combined to reach 0.5cm. Therefore it is required that the result of Equation C.2 be less than 0.25cm. Therefore the equation to optimize is:

$$0.25 \leq \sqrt{\left( \frac{F_{NB_z} l_{arm}}{AE} \right)^2 + \left( \frac{F_{NB_y} l_{arm}^3}{3EI} + \frac{M_{NB} l_{arm}^2}{2EI} \right)^2} \quad (\text{C.3})$$

## C.2 Gondola Arm Fatigue Failure

The loading and unloading of the plastic gondola arm due to the reaction force of the keel on the gondola motor could potentially cause a fatigue failure. A paper on cyclic performance of Laser Sintered Nylon [3] was used to quantify the effects of fatigue on the plastic. Very little research has been done for fatigue failure of 3D printed material. The laser sintering process is similar to 3D printing in that it melts layers of plastic in succession to obtain complex geometries with no pre-existing tooling required. Because of this, the laser sintering process creates shear planes, much like those created in 3D printing. For this reason, the paper was as a basis for the fatigue analysis of the 3D printed part, as these shear planes are critical to the fatigue strength of the material.

The S-N curve shown in Figure C.1 was used to determine the maximum nominal stress that the gondola could take, thus defining the criteria for failure.

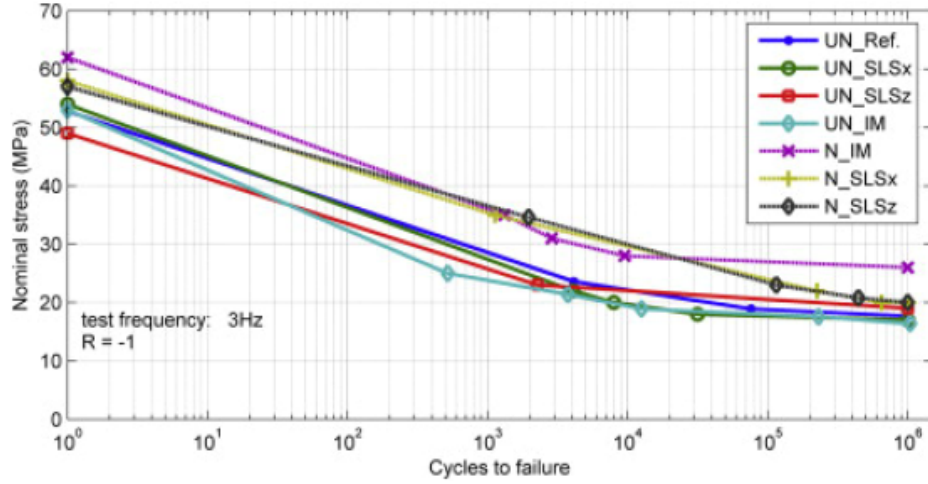


Figure C.1: S-N Curve for Laser Sintered Nylon [3], Used to Determine the Fatigue Failure of the Gondola Body

Assuming that the loading frequency is not higher than around 3hz, no appreciable heat is generated and thus the loading frequency should not affect the cycles to failure. Assuming SLS nylon, the maximum nominal stress for infinite life ( $10^6$  cycles) is  $17MPa$ . Any higher and the part will fail after enough loading cycles.

To find the nominal stress, the amount of stress fluctuation which the gondola arm will sustain needs to be computed. For this, the lowest stress will be when the gondola is not moving, and is only loaded by the weight of the gondola itself. The highest stress will be when the gondola motor is on at full force, at the worst case scenario **DESCRIBED HERE** bending the gondola arm. These both conditions are computed using **ISAAKS SHIT HERE**, and two values of  $F_{NB}$  are found. The difference between the two is the fluctuation of stress.

$$\sigma_{worst} = \underbrace{\left[ \left( \frac{F_{NB_z}}{A} \right) \hat{k} + \left( \frac{F_{NB_y} l_{arm} c}{I} + \frac{M_{NB} c}{I} \right) \hat{j} \right]}_{\text{Worst Case } F_{NB}}, \sigma_{best} = \underbrace{\left[ \left( \frac{F_{NB_z}}{A} \right) \hat{k} + \left( \frac{F_{NB_y} l_{arm} c}{I} + \frac{M_{NB} c}{I} \right) \hat{j} \right]}_{\text{Best Case } F_{NB}} \quad (C.4)$$

The principle stress for each case  $\sigma_a$  is found, and the difference is computed to get the nominal strength, which must be less than  $17MPa$ . Therefore the optimized equation is:

$$17MPa \geq |\sigma_{best} - \sigma_{worst}| \quad (C.5)$$

### C.3 Thruster Arm Adhesion

To connect the carbon fibre arm to the aluminium body which holds the thruster assembly, epoxy will be used. The carbon fibre arm will slide into an aluminium pocket welded to the aluminium thruster plate, as shown in Figure **ADD RENDERED FIGURE HERE.**

The analysis will be conducted by assuming the adhesion surface will be like a double lap joint, shown in Figure C.2 below.

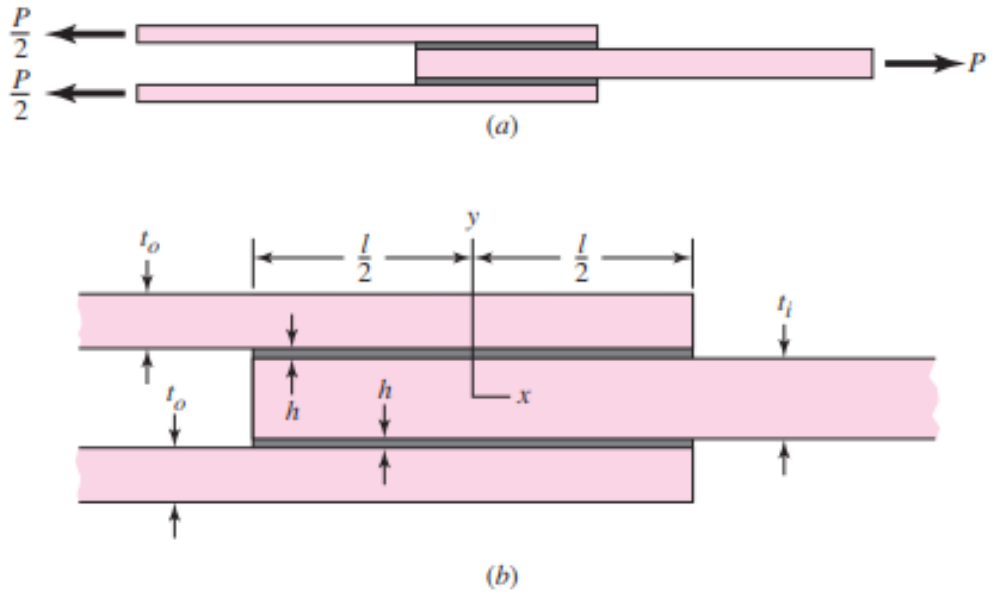


Figure C.2: Analysis of Carbon Fibre Adhesion (From Shigley's Machine Design [5, 484])

The shear-stress distribution of the joint is given by

$$\tau(x) = \frac{P\omega}{4bsinh(\omega l/2)}cosh(\omega x) + \left[ \frac{P\omega}{4bcosh(\omega l/2)} \left( \frac{2E_0t_0 - E_it_i}{2E_0t_0 + E_it_i} \right) + \frac{(\alpha_i - \alpha_0)\Delta T\omega}{(1/E_0t_0 + 2/E_it_i)cosh(\omega l/2)} \right] sinh(\omega x) \quad (C.6)$$

$$\omega = \sqrt{\frac{G}{h} \left( \frac{1}{E_0t_0} + \frac{2}{E_it_i} \right)} \quad (C.7)$$

Where  $E_o$ ,  $t_0$   $\alpha_0$  and  $E_i$ ,  $t_i$   $\alpha_i$  are the modulus, thickness, coefficient of thermal expansion for the outer and inner adherend, respectively.  $G$ ,  $h$ ,  $b$  and  $l$  are the shear modulus, thickness, width and length of the adhesive, respectively.  $\Delta T$  is the change in temperature of the joint, from its curing temperature (zero stress temperature). The closer the curing temperature of the adhesive is to the operating temperature, the lower the thermal stresses induced in the joint will be.

For this case, an unmodified epoxy will be selected as the adhesive material. From [5], Table 9-7, the lap-shear strength can be anywhere from  $10.3 - 27.6 \text{ MPa}$ .  $10.3 \text{ MPa}$  will be selected as a conservative estimate.

The outer material is aluminium and the inner material will be carbon fibre. Because of the nature of aluminium, an extremely thin layer of fibreglass should be added between the carbon fibre and aluminium to prevent corrosion due to the curing of the epoxy. Data was found as follows:

$$\begin{aligned} G &= 1.3 \text{ GPa} [24] \\ E_i &= 109 \text{ GPa} [19] \\ \alpha_i &= 23.7 * 10^{-6} \text{ mm/mm}^\circ\text{C} [19] \\ E_0 &= 71 \text{ GPa} [5] \\ \alpha_0 &= 23.94 \text{ mm/mm}^\circ\text{C} [5] \end{aligned}$$

$\Delta T$  can be estimated by assuming the epoxy is cured at room temperature ( $20^\circ\text{C}$ ) and that the lowest temperature the blimp will be used at is  $-40^\circ\text{C}$ . This yields  $\Delta T = -60^\circ\text{C}$ . The thickness of the adhesive will be estimated as  $h = 0.5 \text{ mm}$ . As preliminary estimates,  $t_0 = 9.73 \text{ mm}$ ,  $t_i = 9.73 \text{ mm}$ ,  $l = 30 \text{ mm}$ , and  $b = 50.80 \text{ mm}$ . The force  $P$  can be estimated using **SOME STUFF**  $P = 100 \text{ N}$ .

Substituting these values into Equation C.7 yields

$$\omega = \sqrt{\frac{1300 \text{ MPa}}{0.5 \text{ mm}} \left( \frac{1}{71000 \text{ MPa} * 9.73 \text{ mm}} + \frac{2}{109000 \text{ MPa} * 9.73 \text{ mm}} \right)} = 0.0930946 \text{ mm}^{-1} \quad (\text{C.8})$$

Followed by substitution into Equation C.6:

$$\begin{aligned} \tau(x) &= \frac{100 \text{ N} * 0.0930946 \text{ mm}^{-1}}{4 * 50.80 \text{ mm} * \sinh(0.0930946 \text{ mm}^{-1} * 30 \text{ mm}/2)} \cosh(0.0930946 \text{ mm}^{-1} * x) + \\ &\left[ \frac{100 \text{ N} * 0.0930946 \text{ mm}^{-1}}{4 * 50.80 \text{ mm} * \cosh(0.0930946 \text{ mm}^{-1} * 30 \text{ mm}/2)} \left( \frac{2 * 71000 \text{ MPa} * 9.73 \text{ mm} - 1300 \text{ MPa} * 9.73 \text{ mm}}{2 * 71000 \text{ MPa} * 9.73 \text{ mm} + 1300 \text{ MPa} * 9.73 \text{ mm}} \right) + \right. \\ &\left. \frac{(23.7 * 10^{-6} \text{ mm/mm}^\circ\text{C} - 23.94 * 10^{-6} \text{ mm/mm}^\circ\text{C}) * (-60^\circ\text{C}) * 0.0930946 \text{ mm}^{-1}}{\left( \frac{1}{71000 \text{ MPa} * 9.73 \text{ mm}} + \frac{2}{109000 \text{ MPa} * 9.73 \text{ mm}} \right) \cosh(0.0930946 \text{ mm}^{-1} * 30 \text{ mm}/2)} \right] \sinh(0.0930946 \text{ mm}^{-1} * x) \\ &= 0.02416 \text{ MPa} * \cosh(0.0930946 \text{ mm}^{-1} * x) + [0.02098 \text{ MPa} + 0.1871 \text{ MPa}] \sinh(0.0930946 \text{ mm}^{-1} * x) \end{aligned} \quad (\text{C.9})$$

at  $x = l/2 = 30 \text{ mm}/2$ , the shear is at a maximum value. Therefore, the shear force is  $\tau = 0.4464 \text{ MPa}$ , Yielding a safety factor of  $\eta = 10.3 \text{ MPa}/0.4464 \text{ MPa} = 23.0734$ .

## C.4 Gondola Motor Shaft

## C.5 Vectoring Shaft Screw Axial Loading Conditions

The screw which secures the nylon vectoring shaft is part of the servo motor assembly. The servo motor output is a spline with a female thread for a 3mm screw to be threaded into (Servo example from ServoCity [28]), as shown in Figure C.3.



Figure C.3: HS-7950TH Servo Spline Attachment [28]

One potential concern would be for the small 3mm screw (which threads into the spline) breaking if an axial load was applied to it. While there is *theoretically* no scenario where any axial load is applied, it is worth checking the strength of the screw, because during transportation of the airship it is possible that the part may be unintentionally pulled. To find the proof force of the bolt, it was assumed that the bolt was a SAE Class 4.8 M3-0.5, and the following properties were found:

Table C.1: Table of Bolt Strength for a M3-0.5 Bolt [2]

RESULTS			
Parameter	Symbol	Value	Unit
Designation	--	M3x0.5	
Property Class	-	4.8	---
Screw Thread Series	--	Coarse	
Nominal Stress Area	$A_{s\_nom}$	5.03	$\text{mm}^2$
Minimum Tensile Strength	$R_m\_{min}$	420	MPa
Minimum Ultimate Tensile Load	-	2110	N
Minimum Stress at 0,2 % non-proportional elongation	$R_{p0.2}\_{min}$	---	MPa
Stress Under Proof Load	$s_p$	310	
Proof Load	-	1560	N
Minimum Breaking Torque	$M_B\_{min}$	---	N.m
Vickers Hardness , $F \geq 98 \text{ N}$	Minimum	130	HV
	Maximum	220	
Minimum Brinell Hardness , $F = 30 \text{ D}^2$	Minimum	124	HBW
	Maximum	209	

Based on this, the tensile load of the bolt is 2110N, which is much higher than any axial forces that the shaft is expected to have to withstand. Therefore the design is not a problem.

## C.6 Vectoring Motor

In order to determine the required torque of the servo that is at the end of the thruster shaft, worst case scenario moments of inertia were considered, as seen in Figure C.4. The angular acceleration can be set

for any chosen servo motor as long as the acceleration is less than the specified maximum. The shaft could be either hollow or solid, therefore the solid case was chosen to account for the higher moment of inertia. The thruster motor and mounting bracket were considered as a single rectangular prism. The propeller was also considered as a rectangular prism.

$$T_{servo} = I_{total} \cdot \alpha \quad (\text{C.10})$$

$$I_{total} = \frac{m_{shaft} \cdot r_{st}^2}{2} + \frac{(m_{motor} + m_{bracket})}{12} \cdot (d_{m_x}^2 + d_{m_z}^2) + \frac{m_{prop}}{12} \cdot (d_{p+x}^2 + d_{p_z}^2) \quad (\text{C.11})$$

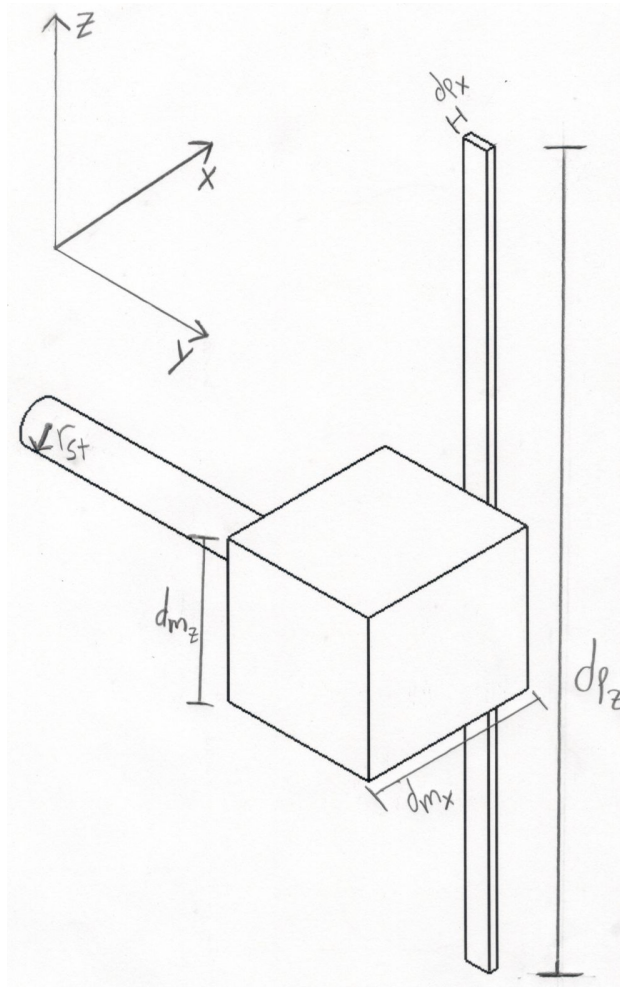


Figure C.4: Thruster Pitching Shaft Worst Case Moment of Inertia

## C.7 Gondola Hinge

The loading on the gondola hinge by forces  $R_{x'}$  and  $R_{z''}$  calculated in system modelling section ?? will be relatively small. Stress concentration would occur at points A and B shown in Figure C.5, however

to avoid these stress concentrations fillets will be added to the part.

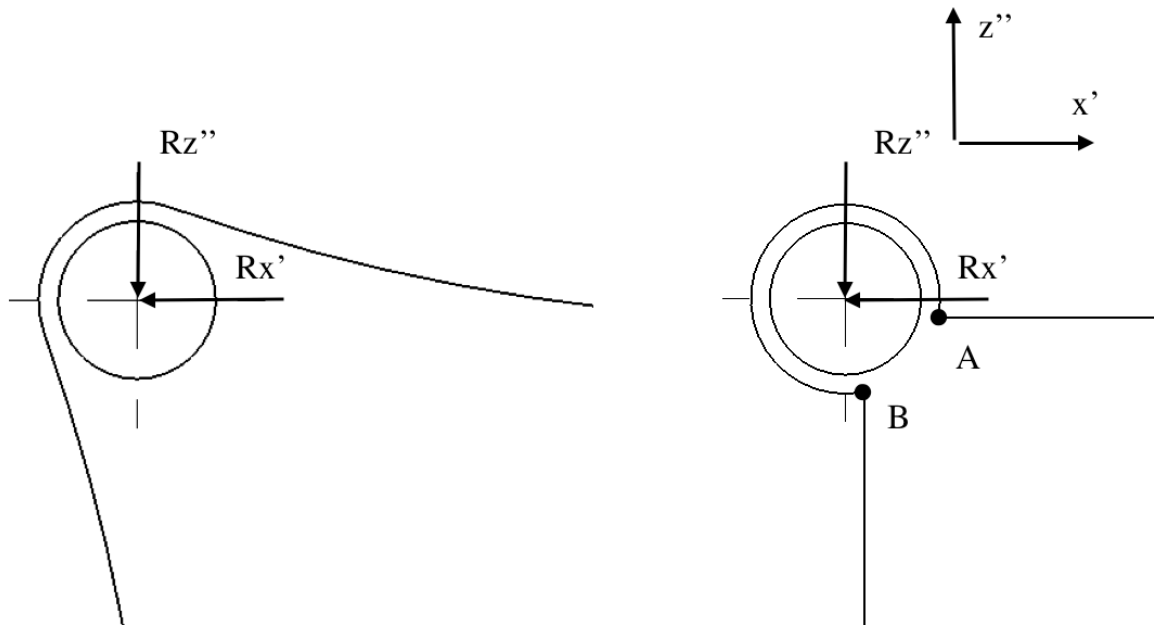


Figure C.5: Gondola Hinge Comparison Fillet Vs. No Fillet

The hinge pin will likely be made of aluminium and the shear stress experienced by the part will not be considerable relative to the strength of the material.

## C.8 Bearings

### C.8.1 Gondola Bearings

### C.8.2 Thruster Bearings

### C.8.3 Thruster Bearings Press Fit

The bearing in the Bearing Shaft Support seen in Figure ?? will be mounted using a press fit. The calculations [7] for will need to be used for the bearing as the hub (shaft into bearing) and as the shaft (bearing into Bearing Shaft Support). These calculations assume similar materials for the hub and shaft.

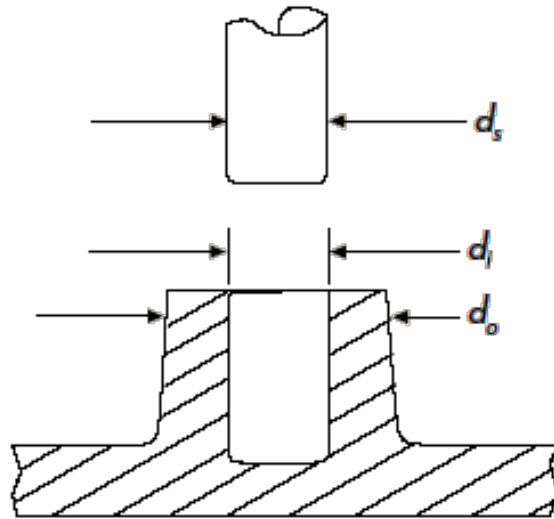


Figure C.6: Pressfit Interference Diameters [7]

$$\sigma_a = \frac{d_s - d_i}{d_s} \cdot E_p \cdot \frac{d_o^2 + d_s^2}{2d_o^2} \quad (\text{C.12})$$

$$i_a = d_s \cdot \frac{\sigma_a}{E_p} \cdot \frac{d_o^2 + d_s^2}{2d_o^2} \quad (\text{C.13})$$

$$n = \frac{S_y}{\sigma_a} \quad (\text{C.14})$$

Dimensions were taken from the first iteration of the design. Yield stress was estimated as 65MPa for the plastic parts.

$$\sigma_a = \frac{6mm - (5.8mm)}{6mm} \cdot 55MPa \cdot \frac{(16mm)^2 + (6mm)^2}{2(16mm)^2} = 1.04MPa$$

$$n = \frac{65MPa}{1.04MPa} = 62.5$$

$$i_a = (6mm) \cdot \frac{(1.04MPa)}{52.6MPa} \cdot \frac{(16mm)^2 + (6mm)^2}{2(16mm)^2} = 0.068mm$$

## C.9 Cauchy Stress Tensor [33]

The Cauchy Stress tensor fully defines the stresses acting on an infinitesimally small element within a material. It is particularly useful for failure analysis, as it is the internal stresses within a material that are used to determine the safety factor of the material at a specific location. Its general forms are shown below.

$$\sigma = \begin{bmatrix} \sigma_{11} & \sigma_{12} & \sigma_{13} \\ \sigma_{21} & \sigma_{22} & \sigma_{23} \\ \sigma_{31} & \sigma_{32} & \sigma_{33} \end{bmatrix} \equiv \begin{bmatrix} \sigma_{xx} & \sigma_{xy} & \sigma_{xz} \\ \sigma_{yx} & \sigma_{yy} & \sigma_{yz} \\ \sigma_{zx} & \sigma_{zy} & \sigma_{zz} \end{bmatrix} \equiv \begin{bmatrix} \sigma_x & \tau_{xy} & \tau_{xz} \\ \tau_{yx} & \sigma_y & \tau_{yz} \\ \tau_{zx} & \tau_{zy} & \sigma_z \end{bmatrix} \quad (\text{C.15})$$

Generally, the use of failure theories requires knowing the *principal stresses*. These are located perpendicular to the *principal planes*. Any body in a state of stress will have three principal planes, where there are no normal shear stresses, only three *principal stresses*.

Any stress tensor can undergo a change of coordinates to obtain the principal stresses. The transformed stress tensor can be written as follows:

$$\sigma' = \begin{bmatrix} \sigma_1 & 0 & 0 \\ 0 & \sigma_2 & 0 \\ 0 & 0 & \sigma_3 \end{bmatrix} \quad (\text{C.16})$$

Obtaining the principle stresses is relatively simple. The principle stresses are simply the eigenvalues of the stress tensor. MATLAB is used to find the eigenvalues of a given stress tensor, and the principle stresses are given by

$$\sigma_1 = \max(\lambda_1, \lambda_2, \lambda_3) \quad (\text{C.17})$$

$$\sigma_3 = \min(\lambda_1, \lambda_2, \lambda_3) \quad (\text{C.18})$$

$$\sigma_2 = \sigma_{11} + \sigma_{22} + \sigma_{33} - \sigma_1 - \sigma_3 \quad (\text{C.19})$$

The principal stresses are then used to conduct failure analysis using the preferred failure analysis method (e.g. Von Mises).

## C.10 Thrust Force

Vectoring thrusters will be mounted to the both sides of the airship via the thruster supports attached to the keel. In order to encompass the forces that will be generated by the thruster, an equation will be used which was developed via research and experimental data collected and compiled by Gabriel Staples [30]. The basis of the equation is Newtons second law.

$$T = \frac{\partial(mv)}{\partial t} = \dot{m}v$$

based on this equation, in theory static thrust can be defined as

$$T_{static} = \dot{m}V_e$$

where  $V_e$  is the escape velocity of air through the thruster in  $m/s$  and  $\dot{m}$  is the mass flow of air through the thruster in  $kg/s$ . For dynamic thrust, which incorporates the movement of the airship,

$$T = \dot{m}\Delta V = \dot{m}(V_e - V_{as})$$

where  $V_{as}$  is the velocity of air coming into the thrusters in  $m/s$  but in a windless circumstance it is the airship velocity. Knowing that  $\dot{m} = \rho A V_e$  and  $A = \pi \frac{D^2}{4}$  where  $A$  is the area the propellers will cover in  $m^2$  and  $D$  is the diameter of the propellers in  $m$ .

$$T = \rho \frac{\pi D^2}{4} (V_e^2 - V_e V_{as}) \quad (\text{C.20})$$

There is obviously some proportionality between the escape velocity  $V_e$  and the tip velocity of the propeller. This claim can be supported by the fact that the tangential velocity of a propeller blade will be increasing along its radius, therefore the greater the diameter the higher the tip speed. This velocity will affect the incident velocity of air it comes into contact with. Therefore a greater diameter will result in greater thrust as well as higher efficiency compared to a propeller of the same pitch with a lesser diameter [30]. This effect however tops out when the tip speed approaches the speed of sound.

Pitch will also affect both the thrust and efficiency. Lower pitch diameter results in lower angle of attack. Lower angle of attack means less separation, less induced drag, as a result, higher diameter and lower pitch props will typically be more efficient [30].

In order to incorporate this into equation C.20,  $V_e$  is replaced with  $V_{pitch}$  which equals  $RPM \cdot Pitch \cdot \frac{1min}{60s}$  where RPM is the rotations per minute of the motor, and Pitch is the pitch di-

ameter of the propeller blade in  $m$ . Equation C.20 is multiplied by a constant coefficient and the propeller diameter to pitch ratio to the power of a constant, as seen below in equation C.21.

$$T = \rho \frac{\pi D^2}{4} \left( K_1 \left( \frac{D}{Pitch} \right)^{K_2} \right) \left( \left( RPM \cdot Pitch \cdot \frac{1min}{60s} \right)^2 - V_{as} \left( RPM \cdot Pitch \cdot \frac{1min}{60s} \right) \right) \quad (\text{C.21})$$

The assumption that  $V_e \approx V_{pitch}$  is not accurate. In addition, it is assumed that the air velocity across the area of the thruster will be constant, when in reality this is not the case [30]. Some of the error derived from these assumptions is corrected by the coefficient term in C.21. In order to choose these coefficients, a study done by Gabriel Staples [30] [29], compares data calculated with equation C.21 using varying constants, with experimental static thrust data from more than 150 tests which were done by multiple sources. These were used along with theoretical dynamic thrust data [4], and a smaller sample of experimental dynamic thrust data. The values for  $K_1$  and  $K_2$  that resulted in calculated thrust forces that best matched the experimental data were 0.16716 and 1.5. Since these values were determined using mainly static thrust data, they are more accurate when calculating static thrust. The highest forces will be generated during low speed or static thrusting so these will be the values used when modeling the parts supporting the thrusters. Results from comparing thrust values calculated using Gabriel Staples's equation C.22 and experimental data for both static and dynamic thrust can be found in appendix section C.10, Figures C.8 and C.9.

The following equation shows a sample calculation using an achievable motor RPM of 11000 from the HobbyKing 2612 Brushless Outrunner Motor 1900KV, whose specs can be seen in appendix section D.8.1. This RPM value was based off results obtained from an online calculator comparing required power values at varying RPMs to the power shown in appendix section C.10, Figures C.10. An airship speed of 10m/s was used.

$$T = \rho \frac{\pi D^2}{4} \left( 0.16716 \left( \frac{D}{Pitch} \right)^{1.5} \right) \left( \left( RPM \cdot Pitch \cdot \frac{1min}{60s} \right)^2 - V_{as} \left( RPM \cdot Pitch \cdot \frac{1min}{60s} \right) \right) \quad (\text{C.22})$$

$$\begin{aligned} &= 1.225[\text{kg/m}^3] \frac{\pi(0.1778[m])^2}{4} \left( 0.16716 \left( \frac{0.1778[m]}{0.127[m]} \right)^{1.5} \right) \left( \left( 11000[\text{rpm}] \cdot 0.127[m] \cdot \frac{1min}{60s} \right)^2 \right. \\ &\quad \left. - 10[m/s] \left( 11000[\text{rpm}] \cdot Pitch \cdot \frac{1min}{60s} \right) \right) = 2.604[N] \end{aligned}$$

Appendix section C.10, Figure C.7 depicts the decrease in thrust force with increasing airship speed. This phenomena can also be observed below in table C.2. At an RPM of 11000 as the air ship reaches 24m/s the thrust force goes to 0 indicating that this would be the maximum speed. Obviously there are several considerable forces such as gravitational forces, drag, and other aerodynamic forces which are not

accounted and this is therefore not an accurate method of determining maximum speed.

Table C.2: Table of Calculated Thrust Values for Varying Airship Speeds

Airship Speed, $V_{as}$ , (m/s)	Airship Speed, $V_{as}$ (mph)	Thrust, T (N)	Thrust, T (g)	Thrust, T (kg)
0	0.000	4.566	465.403	0.465
1	2.237	4.370	445.414	0.445
2	4.474	4.173	425.425	0.425
3	6.711	3.977	405.436	0.405
4	8.948	3.781	385.448	0.385
5	11.185	3.585	365.459	0.365
6	13.422	3.389	345.470	0.345
7	15.659	3.193	325.482	0.325
8	17.896	2.997	305.493	0.305
9	20.132	2.801	285.504	0.286
10	22.369	2.605	265.516	0.266
11	24.606	2.409	245.527	0.246
12	26.843	2.213	225.538	0.226
13	29.080	2.016	205.550	0.206
14	31.317	1.820	185.561	0.186
15	33.554	1.624	165.572	0.166
16	35.791	1.428	145.584	0.146
17	38.028	1.232	125.595	0.126
18	40.265	1.036	105.606	0.106
19	42.502	0.840	85.617	0.086
20	44.739	0.644	65.629	0.066
21	46.976	0.448	45.640	0.046
22	49.213	0.252	25.651	0.026
23	51.450	0.056	5.663	0.006
24	53.687	-0.141	-14.326	-0.014

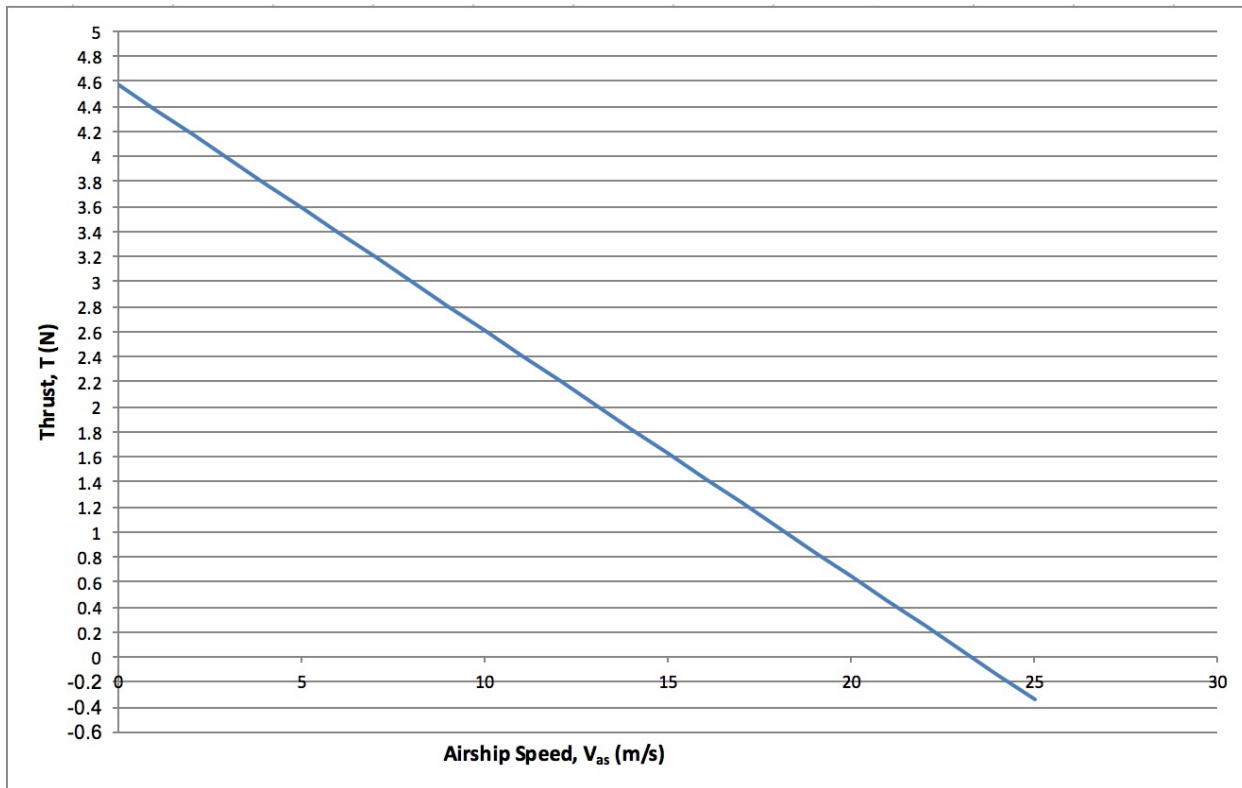


Figure C.7: Graph of Thrust Plotted Against Airship Speed at 11000rpm With 7", 5" Pitch Diameter Propeller

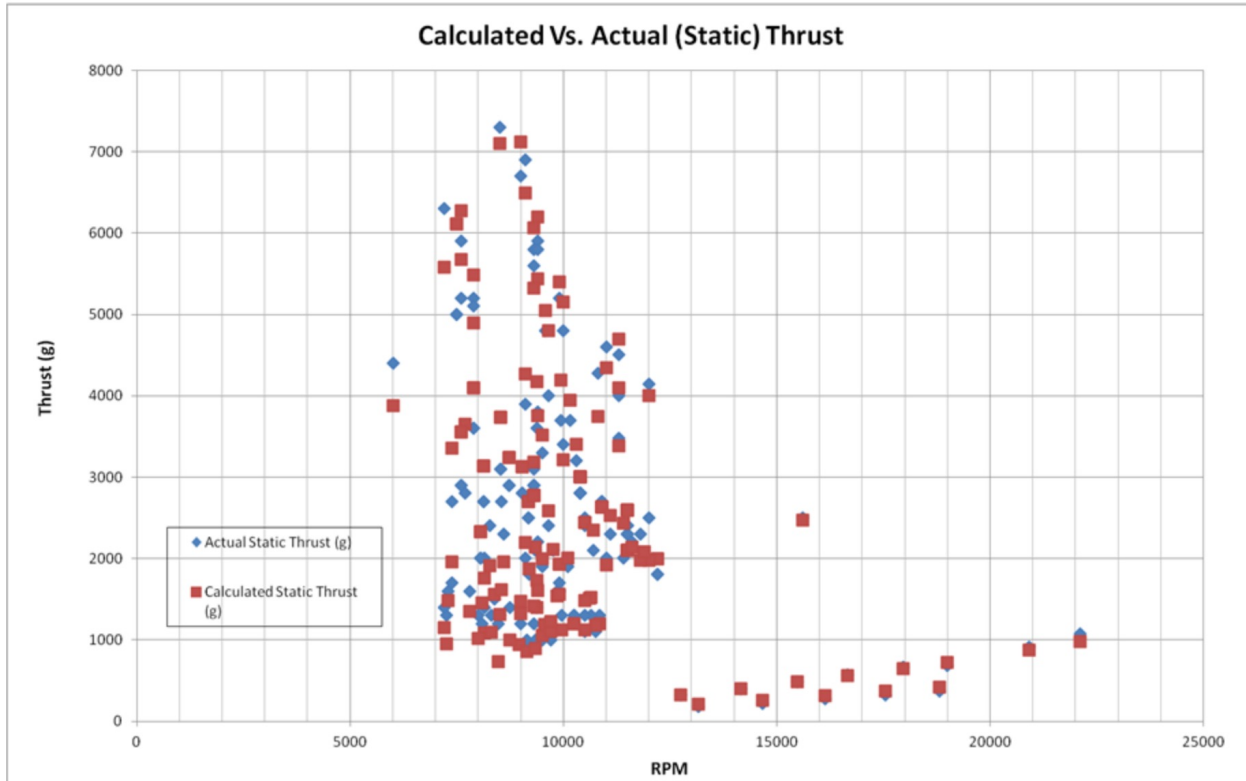


Figure C.8: Test Data from Gabriel Staples Against Experimental Static Thrust Values [30]

### Propeller Dynamic Thrust - Experimental Results vs. Semi-empirical Calculation

10x6 propeller, Full Throttle

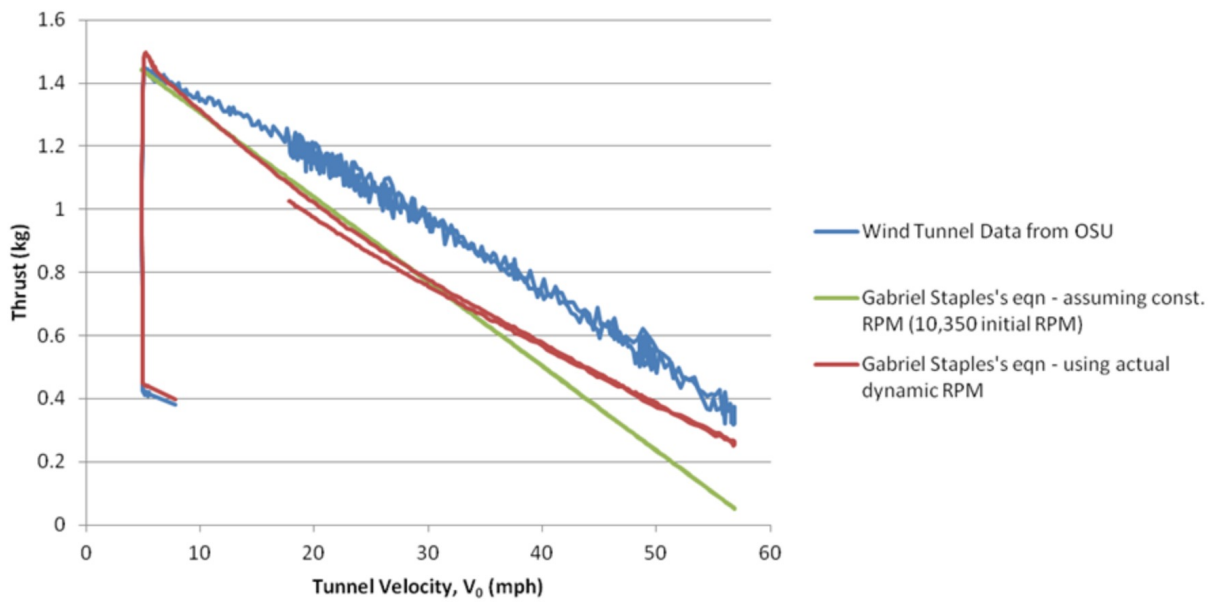


Figure C.9: Test Data from Gabriel Staples Against Experimental Dynamic Thrust Values [30]

Propeller diameter	7	inch
Pitch	5	inch
Propeller type	Standard propeller	
	CF	1
No. of blades	2	<input type="button" value="▼"/>
RPM	11000	
Air temperature	68 Fahrenheit	
Air density	1.2045 (kg/m <sup>3</sup> )	
<b>Static thrust =</b> 12.34 oz		
<b>Static thrust =</b> 0.79 pound		
<b>Static thrust =</b> 0.35 kg		
<b>Perimeter speed =</b> 102.35 m/s		
<b>Required engine power =</b> 0.108 HP = 0.079 kW		
<b>Estimated flying speed =</b> 52.0 mph = 45.1 Knots		

Figure C.10: Sample Thrust Calculation Using On-line Calculator [8]

## C.11 Previous Drag Analysis

Before knowing that the airship envelope needed to be parametrizable, drag values were initially computed using SolidWorks, by its built in Flow Simulation add-on, using a generic airship size. Simulations were conducted from 2m/s to 20m/s, at intervals of 2m/s. Skin Friction Drag and Regular Drag were computed and summed to obtain total drag for each speed. A table with the results from the simulations can be seen in Table C.3.

Table C.3: Raw Data From SolidWorks Flow Simulation

Airspeed (m/s)	Drag Force (N)	Skin Friction Force (N)	Total Drag (N)
2	0.4012	0.0651	0.4663
4	1.5286	0.2035	1.7320
6	3.1225	0.4011	3.5236
8	5.2179	0.7063	5.9242
10	8.2517	1.1397	9.3913
12	12.4647	2.0588	14.5235
14	17.4157	3.9501	21.3659
16	22.8193	5.3402	28.1595
18	29.0603	6.8692	35.9296
20	35.6981	8.4702	44.1682

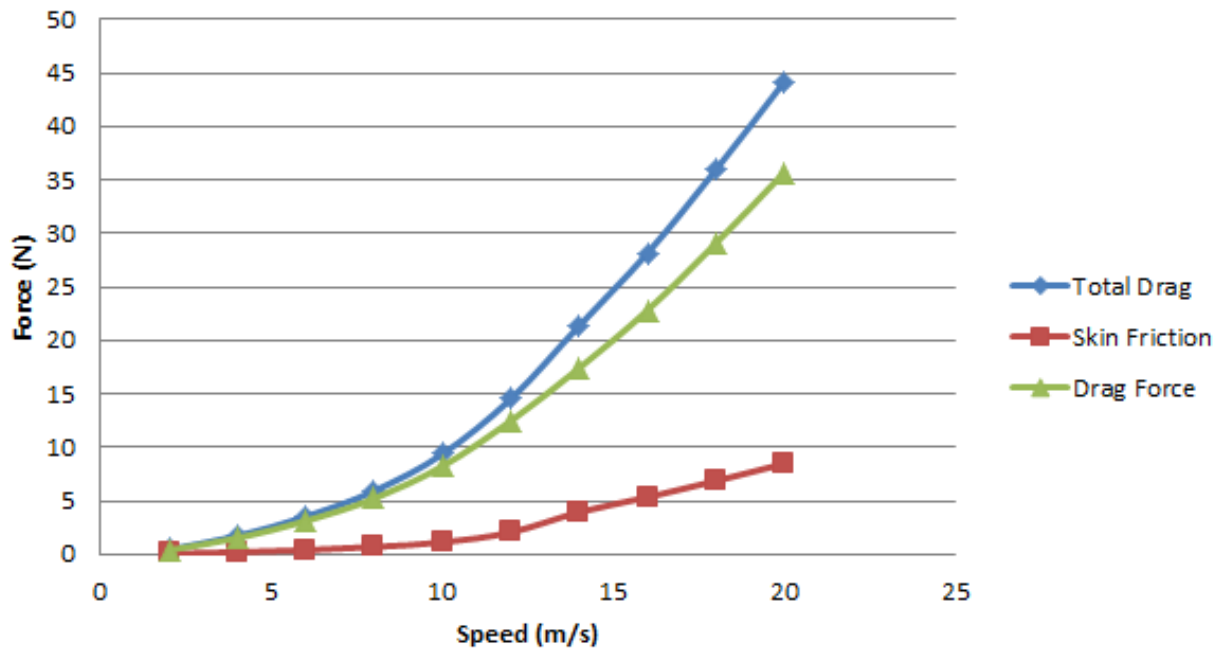


Figure C.11: Drag Force Curves Computed From SolidWorks Flow Simulation

The values of simulated drag were then sent into MATLAB and a curve fitting analysis was completed. A graph of the raw data versus the fitted curve is shown in Figure C.11.

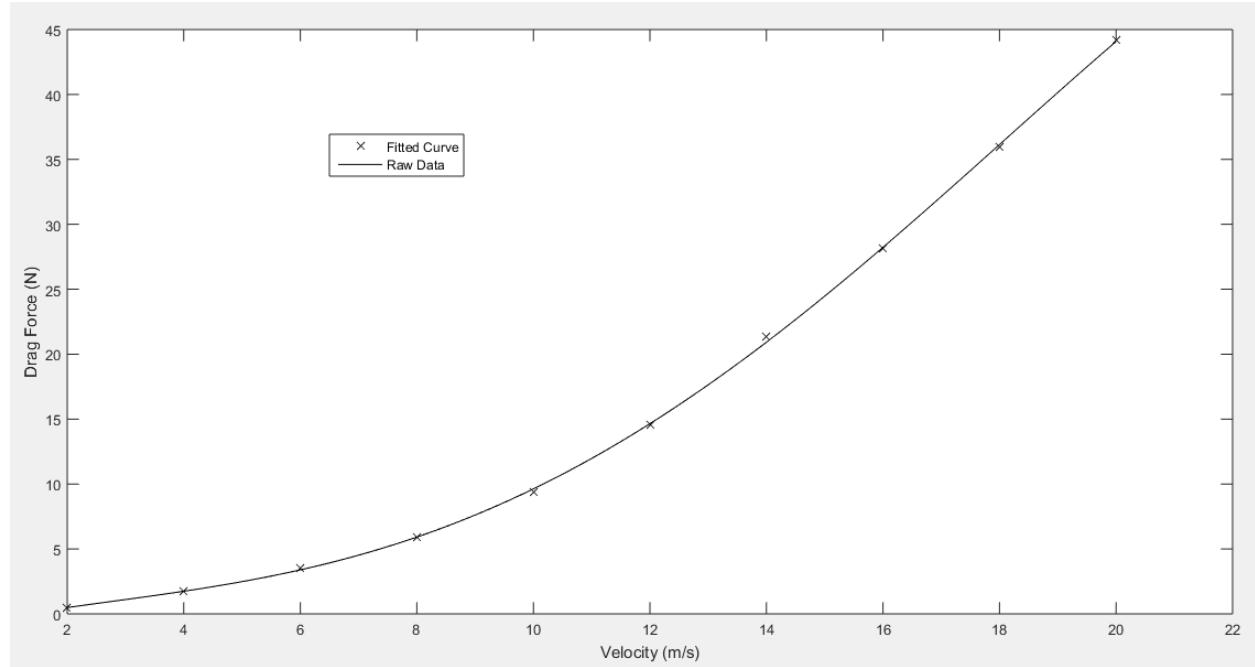


Figure C.12: Drag Force Curves Computed From SolidWorks Flow Simulation

The equation from the curve (generated from MATLAB) was found to be:

$$D(v) = -0.0003545v^4 + 0.014182v^3 - 0.05385v^2 + 0.45054v - 0.087259 \quad (\text{C.23})$$

Where  $D$  is the drag force and  $v$  is the airship speed, in  $m/s$ . Equation C.23 is what is used throughout the report to obtain drag forces.

It is clear that the values computed at here were much higher than that computed from Section ???. This suggests that the program was not outputting reliable results. However, it was found the mesh resolution had a huge impact on the results, as expected, with the value for drag force going from  $44.1682N$  at  $20m/s$  to  $28N$  at  $20m/s$ . The second value, with the more refined mesh, was much closer to the result shown in Section ???, which was  $29.76495N$ .



# Appendix D: Data Sheets

## D.1 Material Properties

### D.1.1 3D Printed Nylon 12 [31]



FDM Nylon 12™ is the first material in Stratasys' new family of nylon offerings, complementing the current portfolio of FDM® materials and enabling new applications requiring: repetitive snap fits, high fatigue resistance, strong chemical resistance and press (friction) fit inserts. Nylon 12 is primarily used in aerospace, automotive and consumer goods industries to take on everything from tooling, jigs and fixtures to covers, panels and vibration resistant components. For use with Fortus 360mc™, 380mc™, 400mc™, 450mc™ and 900mc™ 3D Production Systems, FDM Nylon 12 offers unparalleled toughness and a simple, clean process – free of powders.

MECHANICAL PROPERTIES*	TEST METHOD	ENGLISH		METRIC	
		XZ AXIS	ZX AXIS	XZ AXIS	ZX AXIS
Tensile Strength, Yield (Type 1, 0.125", 0.2"/min)	ASTM D638	4,600 psi	4,100 psi	32 MPa	28 MPa
Tensile Strength, Ultimate (Type 1, 0.125", 0.2"/min)	ASTM D638	6,650 psi	5,600 psi	46 MPa	38.5 MPa
Tensile Modulus (Type 1, 0.125", 0.2"/min)	ASTM D638	186,000 psi	165,000 psi	1,282 MPa	1,138 MPa
Elongation at Break (Type 1, 0.125", 0.2"/min)	ASTM D638	30%	5.4%	30%	5.4%
Elongation at Yield (Type 1, 0.125", 0.2"/min)	ASTM D638	2.4%	2.7%	2.4%	2.7%
Flexural Strength (Method 1, 0.05"/min)	ASTM D790	9,700 psi	8,800 psi	67 MPa	61 MPa
Flexural Modulus (Method 1, 0.05"/min)	ASTM D790	185,000 psi	171,000 psi	1,276 MPa	1,180 MPa
Flexural Strain at Break	ASTM D790	No Break	>10%	No Break	>10%
IZOD impact - notched (Method A, 23°C)	ASTM D256	2.5 ft-lb/in	1 ft-lb/in	135 J/m	53 J/m
IZOD impact - unnotched (Method A, 23°C)	ASTM D256	31 ft-lb/in	3.7 ft-lb/in	1,656 J/m	200 J/m
Compressive Strength, Yield (Method 1, 0.05"/min)	ASTM D695	7,400 psi	7,900 psi	51 MPa	55 MPa
Compressive Strength, Ultimate (Method 1, 0.05"/min)	ASTM D695	24,200 psi	800 psi	167 MPa	6 MPa
Compressive Modulus (Method 1, 0.05"/min)	ASTM D695	730,000 psi	155,000 psi	5,033 MPa	1,069 MPa

UNCONDITIONED (DRY)**					
MECHANICAL PROPERTIES	TEST METHOD	ENGLISH		METRIC	
		XZ AXIS	ZX AXIS	XZ AXIS	ZX AXIS
Tensile Strength, Yield (Type 1, 0.125", 0.2"/min)	ASTM D638	7,700 psi	6,900 psi	53 MPa	48 MPa
Tensile Modulus (Type 1, 0.125", 0.2"/min)	ASTM D638	190,000 psi	180,000 psi	1,310 MPa	1,241 MPa
Elongation at Break (Type 1, 0.125", 0.2"/min)	ASTM D638	9.5%	5%	9.5%	5%
Elongation at Yield (Type 1, 0.125", 0.2"/min)	ASTM D638	6.5%	5%	6.5%	5%
Flexural Strength (Method 1, 0.05"/min)	ASTM D790	10,000 psi	8,600 psi	69 MPa	60 MPa
Flexural Modulus (Method 1, 0.05"/min)	ASTM D790	190,000 psi	180,000 psi	1,300 MPa	1,250 MPa
Flexural Strain at Break	ASTM D790	No Break	>10%	No Break	>10%
IZOD impact - notched (Method A, 23°C)	ASTM D256	2.8 ft-lb/in	0.9 ft-lb/in	150 J/m	50 J/m
IZOD impact - unnotched (Method A, 23°C)	ASTM D256	>37.4 ft-lb/in	5.1 ft-lb/in	>2,000 J/m	275 J/m

STRATASYS.COM

**stratasys**

THE 3D PRINTING SOLUTIONS COMPANY



# FDM Nylon 12

**PRODUCTION-GRADE THERMOPLASTIC FOR  
FORTUS 3D PRODUCTION SYSTEMS**

**At the core:****Advanced FDM Technology**

Fortus 3D Production Systems are powered by FDM (fused deposition modeling) technology. FDM is the industry's leading additive manufacturing technology, and the only one that uses production-grade thermoplastics, enabling the most durable parts. Fortus® systems use a wide range of thermoplastics with advanced mechanical properties so your parts can endure high heat, caustic chemicals, sterilization and high-impact applications.

**No special facilities needed**

You can install a Fortus 3D Production System just about anywhere. No special venting is required because Fortus systems don't produce noxious fumes, chemicals or waste.

**No special skills needed**

Fortus 3D Production Systems are easy to operate and maintain compared to other additive fabrication systems because there are no messy powders to handle and contain. They're so simple, an operator can be trained to operate a Fortus system in less than 30 minutes.

**Get your benchmark on the future of manufacturing**

Fine details. Smooth surface finishes. Accuracy. Strength. The best way to see the advantages of a Fortus 3D Production System is to have your own part built on a Fortus system. Get your free part at: [stratasys.com](http://stratasys.com).

THERMAL PROPERTIES*		TEST METHOD	ENGLISH	METRIC
<b>Heat Deflection (HDT) @ 66 psi annealed</b>		ASTM D648	207°F	97°C
<b>Heat Deflection (HDT) @ 66 psi unannealed</b>		ASTM D648	167°F	75°C
<b>Heat Deflection (HDT) @ 264 psi annealed</b>		ASTM D648	180°F	82°C
<b>Heat Deflection (HDT) @ 264 psi unannealed</b>		ASTM D648	131°F	55°C
<b>Melting Point</b>	-----		352°F	178°C

OTHER	TEST METHOD	VALUE
<b>Specific Gravity</b>	ASTM D792	1.00
<b>Flame Classification</b>	UL94	HB
<b>UL File Number</b>	-----	E345258



SYSTEM AVAILABILITY	LAYER THICKNESS CAPABILITY	SUPPORT MATERIAL	COLOR
<b>Fortus 360mc</b>	0.013 inch (0.330 mm)	SR-110	■ Black
<b>Fortus 380mc</b>	0.010 inch (0.254 mm)		
<b>Fortus 400mc</b>	0.007 inch (0.178 mm)		
<b>Fortus 450mc</b>			
<b>Fortus 900mc</b>			

\*Conditioned = 20°C and 50% RH for 72 hours

\*\*Unconditioned (Dry) = Direct from FDM system

— Annealed = 2 hours @ 140°C

— Unannealed = direct from FDM system

The information presented are typical values intended for reference and comparison purposes only. They should not be used for design specifications or quality control purposes. End-use material performance can be impacted (+/-) by, but not limited to, part design, end-use conditions, test conditions, etc. Actual values will vary with build conditions. Tested parts were built on Fortus 400mc @ 0.010" (0.254 mm) slice. Product specifications are subject to change without notice.

The performance characteristics of these materials may vary according to application, operating conditions, or end use. Each user is responsible for determining that the Stratasys material is safe, lawful, and technically suitable for the intended application, as well as for identifying the proper disposal (or recycling) method consistent with applicable environmental laws and regulations. Stratasys makes no warranties of any kind, express or implied, including, but not limited to, the warranties of merchantability, fitness for a particular use, or warranty against patent infringement.

<sup>1</sup>Literature value unless otherwise noted.

Orientation: See Stratasys Testing white paper for more detailed description of build orientations.



# stratasys®

STRATASYS.COM

ISO 9001:2008 Certified

©2014, 2015, 2017 Stratasys Inc. All rights reserved. Stratasys, FDM, Fortus and Finishing Touch are registered trademarks of Stratasys Inc. FDM Technology, Fused Deposition Modeling, Fortus 250mc, Fortus 380mc, Fortus 400mc, Fortus 450mc, Fortus 900mc, Insight, Control Center, FDM Team, Smart Supports, SR-30, SR-100, ABSplus, ABS-ESD™ and TouchWorks are trademarks of Stratasys, Inc. <sup>1</sup>ULTEM is a trademark of SABIC Innovative Plastics IP BV. All other trademarks are the property of their respective owners, and Stratasys assumes no responsibility with regard to the selection, performance, or use of these non-Stratasys products. Product specifications subject to change without notice. Printed in the USA.MSS\_FDM\_Nylon12\_0317a

**HEADQUARTERS**

7665 Commerce Way, Eden Prairie, MN 55344  
+1 888 480-3548 (US Toll Free)  
+1 952 937-3000 (Intl)  
+1 952 937-0070 (Fax)

2 Holtzman St., Science Park, PO Box 2496  
Rehovot 76124, Israel  
+972 74 745-4000  
+972 74 745-5000 (Fax)

## D.2 Linear Actuator [1]



100mm L12 Actuator  
Actual Size

### Miniature Linear Motion Series • L12

Actuonix Motion Devices unique line of Miniature Linear Actuators enables a new generation of motion-enabled product designs, with capabilities that have never before been combined in a device of this size. These small linear actuators are a superior alternative to designing with awkward gears, motors, servos, and linkages.

Actuonix's L series of micro linear actuators combine the best features of our existing micro actuator families into a highly flexible, configurable, and compact platform with an optional sophisticated on-board microcontroller. The first member of the L series, the L12, is an axial design with a powerful drive-train and a rectangular cross section for increased rigidity. But by far the most attractive feature of this actuator is the broad spectrum of available configurations.

#### L12 Specifications

Gearing Option	50:1	100:1	210:1
Peak Power Point	17N @ 14mm/s	31N @ 7mm/s	62N @ 3.2mm/s
Peak Efficiency Point	10N @ 19mm/s	17N @ 10mm/s	36N @ 4.5mm/s
Max Speed ( <i>no load</i> )	25mm/s	13mm/s	6.5mm/s
Max Force ( <i>lifted</i> )	22N	42N	80N
Back Drive Force ( <i>static</i> )	12N	22N	45N
Stroke Option	10 mm	30mm	50mm
Mass	28 g	34 g	40 g
Repeatability (-I,-R,-P&LAC)	±0.1 mm	±0.2 mm	±0.3 mm
Max Side Load ( <i>extended</i> )	50N	40N	30N
Closed Length ( <i>hole to hole</i> )	62mm	82mm	102mm
Potentiometer (-I, -R, -P)	1kΩ±50%	3kΩ±50%	6kΩ±50%
Voltage Option	6VDC	12VDC	
Max Input Voltage	7.5V	13.5V	
Stall Current	460mA	185mA	
Standby Current (-I/-R)	7.2mA	3.3mA	
Operating Temperature	-10°C to +50°C		
Potentiometer Linearity	Less than 2.00%		
Max Duty Cycle	20 %		
Audible Noise	55dB @ 45cm		
Ingress Protection	IP-54		
Mechanical Backlash	0.2mm		
Limit Switches (-S)	Max. Current Leakage: 8uA		
Maximum Static Force	200N		

1 - Control Option Specific values are identified with -I, -R, -P, -S, and LAC

2 - 1 N (Newton) = 0.225 lbf (pound-force) & 25.4mm=1 Inch

3 - A powered-off actuator will statically hold a force up to the Backdrive Force

4 - Actuators should be tested in each specific application to determine their effective life under those loading conditions and environment.

All information provided on this datasheet is subject to change. Purchase or use of Actuonix actuators is subject to acceptance of our terms and conditions as posted here: <http://www.actuonix.com/terms.asp>

Copyright 2016 © Actuonix Motion Devices Inc.



Actuonix Motion Devices Inc.

580 Starling Lane  
Victoria, BC, V9E 2A9  
Canada

1(206) 347-9684 phone  
1(888) 225-9198 toll-free  
1(206) 347-9684 fax

[sales@actuonix.com](mailto:sales@actuonix.com)  
[www.actuonix.com](http://www.actuonix.com)

## D.3 Bearings [21]

10/10/2017

McMaster-Carr - General Purpose Plastic Ball Bearing, with Stainless Steel Ball, for 1/4" Shaft Diameter, 5/8" OD



### General Purpose Plastic Ball Bearing with Stainless Steel Ball, for 1/4" Shaft Diameter, 5/8" OD

In stock  
\$6.03 Each  
6455K2



Bearing Type	Ball
For Load Direction	Radial
Ball Bearing Type	Standard
Construction	Single Row
Seal Type	Open
For Shaft Shape	Round
Trade No.	R4
For Shaft Diameter	1/4"
ID	0.25"
ID Tolerance	0" to 0.003"
OD	5/8"
OD Tolerance	-0.003" to 0"
Width	0.196"
Width Tolerance	-0.005" to 0.005"
Material	Acetal
Cage Material	Plastic
Radial Load Capacity, lbs.	
Dynamic	25
Static	15
Maximum Speed	2,300 rpm
Shaft Mount Type	Press Fit
Lubrication	Not Required
Temperature Range	-40° to 180° F
ABEC Rating	Not Rated
Radial Clearance	0.001" to 0.008"
Ball Material	Stainless Steel
RoHS	Compliant

Choose these acetal bearings for their all-around corrosion and chemical resistance.

Stainless steel balls offer excellent corrosion resistance.

## D.4 Friction Wheel Assembly

### D.4.1 Friction Wheel [20]

10/10/2017

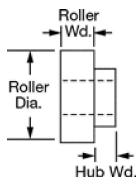
McMaster-Carr - Neoprene Roller, Drive, Aluminum Hub, 5/8" Roller Diameter, 3/16" Roller Width



#### Neoprene Roller

Drive, Aluminum Hub, 5/8" Roller Diameter, 3/16" Roller Width

In stock  
\$16.70 Each  
60885K31



Guide Roller Type	Drive
Roller Style	Shaft Mount
Roller Profile	Flat
Roller Material	Neoprene
Hub Material	Aluminum
Roller	
Diameter	5/8"
Width	3/16"
For Shaft Diameter	1/4"
Hub	
Diameter	1/2"
Width	1/4"
Shaft Mount Type	Set Screw
Set Screws	
Number Required	1
Included	No
Thread Size	8-32
Temperature Range	-40° to 170° F
Durometer (Hardness Rating)	55A (Medium) Black
RoHS	Compliant
Related Product	<a href="#">8-32 Stainless Steel Cup Point Set Screws (100/Pkg.)</a>

Made of neoprene rubber, these rollers resist oil, flames, gasoline, and weather. Also known as contact wheels and feed rollers, they have tapped hubs that allow you to mount them onto a shaft or stud to transmit power.

## D.4.2 Friction Wheel Set Screw [22]

10/10/2017

McMaster-Carr - Alloy Steel Cup-Point Set Screw, Black Oxide, 8-32 Thread, 1/4" Long



### Alloy Steel Cup-Point Set Screw Black Oxide, 8-32 Thread, 1/4" Long

In stock  
\$10.65 per pack of 100  
91375A190



Material	Black-Oxide Alloy Steel
Thread Size	8-32
Length	1/4"
Drive Size	5/64"
Screw Size Decimal Equivalent	0.164"
Hardness	Rockwell C45
Specifications Met	ASME B18.3, ASTM F912
Thread Type	UNC
Thread Spacing	Coarse
Thread Fit	Class 3A
Thread Direction	Right Hand
Drive Style	Hex
Tip Type	Cup
Head Type	Headless
System of Measurement	Inch
RoHS	Compliant

Made from alloy steel, these set screws have a thin edge that digs into hard surfaces for a secure hold. Length listed is the overall length.

Black-oxide alloy steel set screws resist corrosion in dry environments.

### D.4.3 Friction Wheel Motor [25]

10/10/2017

Pololu - 50:1 Micro Metal Gearmotor HP 6V

#### 50:1 Micro Metal Gearmotor HP 6V



www.pololu.com

Pololu item #: 998      438 in stock

Price break	Unit price (US\$)
1	15.95
10	13.55
50	11.96

Quantity:  Add to cart[backorders allowed](#) Add to wish list

This gearmotor is a miniature **high-power, 6 V** brushed DC motor with a **51.45:1** metal gearbox. It has a cross section of 10 × 12 mm, and the D-shaped gearbox output shaft is 9 mm long and 3 mm in diameter.

**Key specs at 6 V:** 625 RPM and 120 mA with no load, 15 oz-in (1.1 kg-cm) and 1.6 A at stall.

Select options:

[Description](#)   [Specs \(10\)](#)   [Pictures \(20\)](#)   [Resources \(12\)](#)   [FAQs \(1\)](#)   [On the blog \(1\)](#)

#### Dimensions

<b>Size:</b>	10 × 12 × 26 mm <sup>1</sup>
<b>Weight:</b>	9.5 g
<b>Shaft diameter:</b>	3 mm <sup>2</sup>

#### General specifications

<b>Gear ratio:</b>	51.45:1
<b>Free-run speed @ 6V:</b>	630 rpm
<b>Free-run current @ 6V:</b>	120 mA
<b>Stall current @ 6V:</b>	1600 mA
<b>Stall torque @ 6V:</b>	15 oz·in
<b>Extended motor shaft?:</b>	N

<https://www.pololu.com/product/998/specs>

1/2

Table D.1: Various Gearing For Gondola Motor Torque [25].

<b>6 V</b>	high-power <b>(HP)</b> <i>(same specs as 6V HPCB above)</i>	1600 mA	6000 RPM	2 oz-in	<u>5:1 HP 6V</u>	<u>5:1 HP 6V dual-shaft</u>
			3000 RPM	4 oz-in	<u>10:1 HP 6V</u>	<u>10:1 HP 6V dual-shaft</u>
			1000 RPM	9 oz-in	<u>30:1 HP 6V</u>	<u>30:1 HP 6V dual-shaft</u>
			625 RPM	15 oz-in	<u>50:1 HP 6V</u>	<u>50:1 HP 6V dual-shaft</u>
			400 RPM	22 oz-in	<u>75:1 HP 6V</u>	<u>75:1 HP 6V dual-shaft</u>
			320 RPM	30 oz-in	<u>100:1 HP 6V</u>	<u>100:1 HP 6V dual-shaft</u>
			200 RPM	40 oz-in	<u>150:1 HP 6V</u>	<u>150:1 HP 6V dual-shaft</u>
			140 RPM	50 oz-in	<u>210:1 HP 6V</u>	<u>210:1 HP 6V dual-shaft</u>
			120 RPM	60 oz-in	<u>250:1 HP 6V</u>	<u>250:1 HP 6V dual-shaft</u>
			100 RPM	70 oz-in	<u>298:1 HP 6V</u>	<u>298:1 HP 6V dual-shaft</u>
			32 RPM	125 oz-in	<u>1000:1 HP 6V</u>	<u>1000:1 HP 6V dual-shaft</u>

### D.4.4 Friction Wheel Encoder [26]

10/10/2017

Pololu - Magnetic Encoder Pair Kit for Micro Metal Gearmotors, 12 CPR, 2.7-18V (HPCB compatible)

#### Magnetic Encoder Pair Kit for Micro Metal Gearmotors, 12 CPR, 2.7-18V (HPCB compatible)

**Pololu item #:** 3081    **574** in stock

Price break	Unit price (US\$)
1	8.95
10	7.95
50	6.95

**Quantity:**  **Add to cart**

**backorders allowed** **Add to wish list**

Navigation icons: back, forward, search.

Add quadrature encoders to your micro metal gearmotors (extended back shaft version required) with this kit that uses a magnetic disc and hall effect sensors to provide 12 counts per revolution of the motor shaft. The sensors operate from 2.7 V to 18 V and provide digital outputs that can be connected directly to a microcontroller or other digital circuit. This module is compatible with **all** of the dual-shaft micro metal gearmotors we carry, including the HPCB versions.

[Description](#)   [Specs \(6\)](#)   [Pictures \(13\)](#)   [Resources \(5\)](#)   [FAQs \(0\)](#)   [On the blog \(4\)](#)

#### Overview

This kit includes two dual-channel Hall Effect sensor boards and two **6-pole magnetic discs** that can be used to add quadrature encoding to two **micro metal gearmotors with extended back shafts** (motors are not included with this kit). The encoder board senses the rotation of the magnetic disc and provides a resolution of 12 counts per revolution of the motor shaft when counting both edges of both channels. To compute the counts per revolution of the gearbox output shaft, multiply the gear ratio by 12.

### D.4.5 Example Cable Gland [18]



<b>DATA SHEET</b>	53111000
<b>SKINTOP® ST-M / STR-M</b>	valid from : 21.07.2017

The polyamide based SKINTOP® ST-M / STR-M is designed for universal use, above all for functional safety in manufacturing of machines and equipment, in measurement and control technology and automation technology, as well as in the electronic technology and in manufacturing of robots.



#### Components:

Gland body	Polyamide, V-2 acc. to UL 94
Cap nut	Polyamide, V-2 acc. to UL 94
Sealing ring	CR (ozone- and UV-resistant)
O-Ring (M40x1,5 - M63x1,5)	NBR (ozone- and UV-resistant)

#### Technical features:

Connecting thread	M12x1,5 up to M63x1,5 acc. to EN 60423
Functional thread	Multi-start trapezoidal thread
Protection class IP / NEMA Enclosure types	IP68 – 5 bar/30 min, test acc. to EN 60529 IP69 acc. to EN 60529 NEMA Type 1 and Type 12
Strain relief:	Kat. A acc. to DIN EN 62444
Temperature range:	Dynamic -20 °C up to +100 °C Statically -40 °C up to +100 °C
Design	ST-M standard STR-M with reducing sealing ring (for smaller cable diameters)
Colour	RAL 7001 silver-grey RAL 7035 light-grey RAL 9005 black, UV-resistant

#### Other characteristics:

Permanent vibration protection  
Optimal strain relief  
Large variable clamping ranges  
M40 - M63 with O-ring

#### Approvals:



File Nr. 79903

#### Norm references:

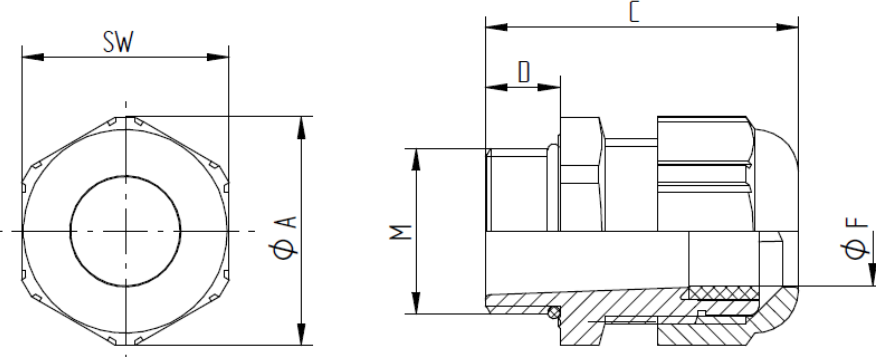


For more information please see our current catalogue.

elaborated by: PDP: T. Dvoulety	Document: DB53111000_11EN	page 1 of 2
------------------------------------	---------------------------	-------------



<b>DATA SHEET</b>		53111000
SKINTOP® ST-M / STR-M		valid from : 21.07.2017



#### SKINTOP® ST-M

M	SW [mm]	Ø A [mm]	C [mm]		D [mm]	Ø F [mm] Clamping range	O-Ring [mm]	Article No.		
			min.	max.				RAL 7001	RAL 7035	RAL 9005
M12x1,5	15	16,6	26,5	30	8	3,5 - 7	-	53111000	53111400	53111200
M16x1,5	19	21,1	29	34	8	4 - 10	-	53111010	53111410	53111210
M20x1,5	25	27,6	34	37	9	6 - 13	-	53111020	53111420	53111220
M25x1,5	30	33,6	35	40	10	8 - 17	-	53111030	53111430	53111230
M32x1,5	36	40,3	39	47	10	9 - 21	-	53111040	53111440	53111240
M40x1,5	46	51,6	43	52	10	16 - 28	36 x 2	53111050	53111450	53111250
M50x1,5	55	61,6	54	62	12	27 - 34	46 x 2	53111060	53111460	53111260
M63x1,5	66	73,9	59	71	12	34 - 45	57 x 2	53111070	53111470	53111270

#### SKINTOP® STR-M

M	SW [mm]	Ø A [mm]	C [mm]		D [mm]	Ø F [mm] Clamping range	O-Ring [mm]	Article No.		
			min.	max.				RAL 7001	RAL 7035	RAL 9005
M12x1,5	15	16,6	26,5	30	8	2 - 5	-	53111100	53111500	53111300
M16x1,5	19	21,1	29	34	8	3,5 - 7	-	53111110	53111510	53111310
M20x1,5	25	27,6	34	37	9	4 - 10	-	53111120	53111520	53111320
M25x1,5	30	33,6	35	40	10	5 - 13	-	53111130	53111530	53111330
M32x1,5	36	40,3	39	47	10	6 - 15	-	53111140	53111540	53111340
M40x1,5	46	51,6	43	52	10	9 - 23	36 x 2	53111150	53111550	53111350
M50x1,5	55	61,6	54	62	12	24 - 29	46 x 2	53111160	53111560	53111360
M63x1,5	66	73,9	59	71	12	28 - 39	57 x 2	53111170	53111570	53111370

elaborated by: PDP: T. Dvoulety	Document:	DB53111000_11EN	page 2 of 2
------------------------------------	-----------	-----------------	-------------

## D.5 Keel Construction Quote

									
Order No.: XYPQ-170922-02				Date : Sep,22th, 2017					
<b>SUPPLIER:</b>									
Sale Executive: Patrick XY Electronics Technology Co.,Ltd Off Add: Room 405, LiJinCheng Bulding, Jihua Road, Longhua new district,Shenzhen. Email: sales890@xy-global.com Tel: 0086-755-8273-7469    Fax: 0086-755-8273-7710									
<b>CUSTOMER:</b>									
Name: Sawyer Woodside									
<b>Quotation</b>									
Item	Drawing No.	Photo	Description	Quantity (pcs)	Unit Price (USD)	Amount (USD)			
Tooling cost for straight rod	N/A	N/A	Tooling cost, including 2 pcs of samples	1.00	1213.00	1213.00			
Tooling cost for curved rod	N/A	N/A	Tooling cost, including 1 pcs of sample	1.00	1970.00	1970.00			
Straight rod	N/A		Material: Carbon fiber, 2 mm thick. Dimension: 1 m in length.	1.00	15.79	15.79			
Curved rod	N/A		Material: Carbon fiber, 2 mm thick. Dimension: 1 m in length, curved to 90° .	1.00	23.69	23.69			
1. All of the above quotation based on USD.									
2. Payment: A) Mold fee : T/T 50% deposit in advance, 50% of balance after sample are confirmed; B) Goods : T/T 30% deposit in advance, 70% balance before shipment.									
3. Price Terms: EX Work, Shenzhen.									
4. Lead time: 30 days									
5. When the price fluctuation for raw material exceed 3%,the price need be reconfirmed.									
6. The quotation is based on the drawing ,the two parties need to confirm the drawing when production begin.									
7. Packing: Carton Package.									
8. This quotation is valid until Oct. 21st, Beijing time.									

## D.6 Spring [23]

10/10/2017

McMaster-Carr - Music-Wire Steel Torsion Spring, 180 Degree Right-Hand Wound, 0.767" OD



### Music-Wire Steel Torsion Spring 180 Degree Right-Hand Wound, 0.767" OD

In stock  
\$8.06 per pack of 6  
9271K271



Spring Type	Torsion
Material	Music-Wire Steel
Deflection Angle	180°
Wind Direction	Right Hand
OD	0.767"
For Maximum Shaft Diameter	0.500"
Wire Diameter	0.063"
Leg Length	2,000"
Number of Coils	6.00
Spring Length @ Maximum Torque	0.475"
Maximum Torque	5,518 in.-lbs.
RoHS	Compliant

These music-wire steel springs are stronger than stainless steel springs. Commonly found in clothespins, spring clamps, mousetraps, motors, and spring-return mechanisms, torsion springs maintain pressure over a short distance in a rotational direction. They are often supported by a shaft, mandrel, or arbor.

Squeezing a torsion spring reduces its OD, which tightens the spring around a shaft and increases the spring length. Since the spring gets tighter as it is squeezed around the shaft, a maximum shaft diameter for each spring is listed. Using a shaft with a larger diameter will interfere with the spring motion.

Torsion springs should be used in the direction in which the coils are wound. Deflection angle represents the angle between the legs of the spring as well as the maximum spring rotation. All springs rotate until their legs are parallel. For example, a spring with a 90° deflection angle has a 90° angle between its legs, and it will rotate a maximum of 90°. Maximum torque is the torque required to rotate the spring legs to the parallel position.

## D.7 Battery [9]

Rhino 2250mAh 3S 11.1v 40C Lipoly Pack



### Specifications

SKU:	R2250-40-3	Brand:	N/A
Weight(g)	243.00	Length	109.00
Width:	26.00	Height:	36.00
Capacity (mAh)	2250.00	Discharge(c)	40.00
Length-A(mm):	107.00	Height-B(mm):	34.00
Width-C(mm)	26.00	Unit Weight (g)	191
Max Charge Rate(C):	5.00	Discharge Plug:	N/A

## D.8 Thruster Assembly

### D.8.1 Thruster Motor [16]

HobbyKing®™ 2612 Brushless Outrunner 1900KV



#### Specifications

RPM/V: **1900Kv**  
Cell Count: **2~3s Lipoly**  
Max.efficiency: **78.0%**  
Current at Max.eff: **6.3~8.7A**  
Max.current: **14A**  
No Load Current: **0.8A/7V**  
Internal Resistance: **165mOhm**  
Diameter: **27mm**  
Length: **23.4mm**  
Mounting Hole Spacings: **32mm**  
Mounting Hole Diameter: **2mm**  
Shaft: **3mm**  
Weight: **25g**

### D.8.2 Propeller [14]

Aerostar Carbon Fibre Propeller 7x5



#### Specifications

SKU:	9445000180-0	Brand:	N/A
Weight(g)	14.00	Length	180.00
Width:	15.00	Height:	20.00
Pitch Y(inch)	5.00	Material	Carbon Fiber
Rotation:	CCW	Unit Weight (g):	N/A
Type	Normal	Blade Count	2
Diameter X(inch):	7.00		

### D.8.3 BEC [10]

#### TURNIGY Plush 10amp Speed Controller w/BEC



#### Specifications

Cont Current: <b>10A</b>	SKU:	TR_P10A
Burst Current: <b>12A</b>	Weight(g)	20.00
BEC Mode: <b>Linear</b>	Width:	10.00
BEC : <b>5v / 2A</b>	Brand:	No
Lipo Cells: <b>2-4</b>	Length	110.00
NiMH : <b>5-12</b>	Height:	110.00
Weight: <b>9g</b>		
Size: <b>27x17x6mm</b>		

## D.8.4 Servo Motor [27]

**RB-Hit-128**

**HS-7950TH Ultra Torque HV Coreless Titanium Gear Servo**



Hitec's strongest servo period, the "Ultra Torque" HS-7950TH is designed to operate on a two cell LiPo Pack. Featuring our high resolution "G2" second generation programmable digital circuit and our indestructible Titanium gears, the HS-7950TH has the performance and durability you've come to expect from a Hitec servo. Other features in the HS-7950TH include a 7.4V optimized coreless motor, integrated heat sink case, and a top case with two hardened steel gear pins supported by axial brass bushing.

The HS-7950TH has been designed for the most demanding hobby applications including the largest aircraft and monster trucks. Featuring a titanic 403 oz./in. of torque at 6.0 volts, while still maintaining a respectable 0.15 second transit time.

### Features

- G2 Digital Circuit
- Titanium Gear Train (MK first gear)

- Ultra Performance Coreless Motor
- Heatsink Case
- (8) O-Rings for Water/Dust/Fuel protection
- Dual Ball Bearing Supported Output Shaft

**Programmable Features Include:**

- Dead Band Width
- Direction of Rotation
- Speed of Rotation (slower)
- End Points
- Neutral Points
- Fail Safe On/Off
- Fail Safe Point
- Resolution\* (default is high resolution)
- Overload Protection\* (default is off)

**Specifications**

- Motor Type: Coreless
- Bearing Type: Dual Ball Bearing
- Speed (6.0V/7.4V): 0.15 / 0.13
- Torque oz./in. (6.0V/7.4V): 403 / 486
- Torque kg./cm. (6.0V/7.4V): 29.0 / 35.0
- Size in Inches: 1.57 x 0.79 x 1.50
- Size in Millimeters: 39.88 x 20.07 x 38.10
- Weight oz.: 2.40
- Weight g.: 68.04

### D.8.5 Receiver [15]

FrSky TFR6M 2.4Ghz 6CH Micro Receiver FASST Compatible



#### Specification

SKU:	236000003	Brand:	FrSky
Weight(g)	34.00	Length	160.00
Width:	20.00	Height:	87.00

## D.9 Flight Control Assembly

### D.9.1 ESC [11]

Turnigy 20A BRUSHED ESC



#### Specifications

SKU:	TGY-20A	Brand:	No
Weight(g)	39.00	Length	150.00
Width:	10.00	Height:	110.00

### D.9.2 GPS Module [13]

UBLOX Micro M8N GPS Compass Module

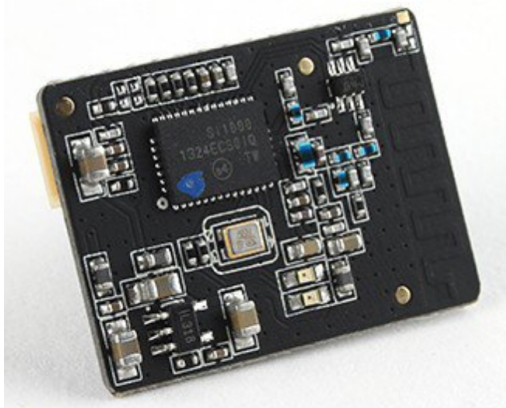


#### Specifications

SKU:	9387000083-0	Brand:	No
Weight(g)	29.00	Length	80.00
Width:	10.00	Height:	60.00

### D.9.3 Transceiver [17]

Micro HKPilot Telemetry Radio Set with Integrated PCB  
Antenna 915Mhz



#### Specifications

Supply voltage: **3.7-6 VDC**

Transmit current: **100 mA at 20 dBm**

Receive current: **25 mA**

Serial interface: **3.3 V UART**

Size: **19x25x5mm (with antenna)**

Weight: **1.6g (with antenna)**

#### Specs Ground Transceiver:

Supply voltage: **3.7-6 VDC (from USB or DF13 connector)**

Transmit current: **100 mA at 20 dBm**

Receive current: **25 mA**

Serial interface: **3.3 V UART**

Size: **25.5x 53x11 mm (without antenna)**

Weight: **11.5g (without antenna)**

SKU:	387000067-0	Brand:	No
Weight(g)	44.00	Length	100.00
Width:	40.00	Height:	70.00

#### D.9.4 Flight Controller [12]

PixFalcon Micro PX4 Autopilot



##### Specifications

SKU:	9387000082-0	Brand:	N/A
Weight(g)	99.00	Length	107.00
Width:	40.00	Height:	74.00

# **Appendix E: Engineering Drawings**

## **E.1 Parts List**

## **E.2 Complete System Drawing**

including cross sections

## **E.3 Sub-Assembly Drawings**

## **E.4 Individual Part Drawings**



# Appendix F: Meeting Minutes

## F.1 Group Meeting Minutes

<b>Group Minutes</b>					
<b>Attendees:</b> Alex Pennell (apenn095@uottawa.ca,7334789) Isaak Goldenberg (igold093@uottawa.ca,7395188) Joey Kane (jkane035@uottawa.ca,7386330) Sawyer Woodside (swood079@uottawa.ca,7158568)		<b>Absent:</b> none	<b>Date &amp; Time:</b> 10:30 am 6-Sept-2017	<b>Venue:</b> CBYB02	
<b>Minute taker:</b> Sawyer Woodside Who is filling out this form?			<b>Chairperson:</b> Who is organising the meeting?	<b>Sawyer Woodside</b>	
	<b>Task</b> What has to be done?	<b>Action</b> What action is required to get it done?	<b>Who</b> Who is responsible?	<b>Duration</b> How long will it take to complete?	<b>Status</b> Has the task been completed?
<b>1</b>	Formatting Report	Pick software, organize template	Joey, Isaak	2 hours	No
<b>2</b>	Find Images	Write descriptions of the different parts, function, history, etc.	All	Ongoing	No
<b>3</b>	Filing	Set up a Google drive	Alex	1 hour	Yes
<b>4</b>	Meeting and Minutes	Decided chair person and taker are the same. Weekly rotation, setup schedule.	Sawyer	1 hour	Yes
<b>5</b>	Messaging	Setup Slack software	Sawyer	10 minutes	Yes
<b>Next meeting</b> Chairperson: <b>Sawyer Woodside</b>	<b>Minute taker:</b> <b>Sawyer Woodside</b>	<b>Date &amp; Time:</b> 11:30am 8-Sept-2017	<b>Venue:</b> <b>CBY B02</b>		

<b>Group Minutes</b>					
<b>Attendees:</b> Alex Pennell (apenn095@uottawa.ca,7334789) Isaak Goldenberg (igold093@uottawa.ca,7395188) Joey Kane (jkane035@uottawa.ca,7386330)		<b>Absent:</b> Sawyer Woodside	<b>Date &amp; Time:</b> 08:30 am 13-Sept-2017	<b>Venue:</b> CBYB02	
<b>Minute taker:</b> Who is filling out this form? Alex Pennell		<b>Chairperson:</b> Who is organising the meeting? <b>Alex Pennell</b>			
	<b>Task</b> What has to be done?	<b>Action</b> What action is required to get it done?	<b>Who</b> Who is responsible?	<b>Duration</b> How long will it take to complete?	<b>Status</b> Has the task been completed?
<b>1</b>	Read through other blimp designs	Use the references in the journal to find other designs	Joey	4 Hours	In progress
<b>2</b>	Write section on basic design	Find relevant pictures to use as reference and put in document	Isaak	6 Hours	In progress
<b>3</b>	Research attaching the gondola to keel and how it can move	Find relevant picture	Alex	6 Hours	In progress
<b>4</b>	Research and summarize regulations	Read through FAA guidelines for airships	Sawyer	6 Hours	In progress
<b>5</b>	Write scope and mandate	Start and finish the scope and mandate	Isaak	2 Hours	Complete
<b>Next meeting</b> <b>Chairperson:</b> <b>Alex Pennell</b>	<b>Minute taker:</b> <b>Alex Pennell</b>		<b>Date &amp; Time:</b> 11:30am 13-Sept-2017	<b>Venue:</b> <b>CBY B02</b>	

<b>Group Minutes</b>					
<b>Attendees:</b> Alex Pennell (apenn095@uottawa.ca,7334789) Isaak Goldenberg (igold093@uottawa.ca,7395188) Joey Kane (jkane035@uottawa.ca,7386330) Sawyer Woodside (swood079@uottawa.ca,7158568)		<b>Absent:</b> none	<b>Date &amp; Time:</b> 11:30 am 19-Sept-2017	<b>Venue:</b> DMS	
<b>Minute taker:</b> Isaak Goldenberg Who is filling out this form?		<b>Chairperson:</b> Who is organising the meeting?	Alex Pennell		
<b>Task</b> What has to be done?	<b>Action</b> What action is required to get it done?	<b>Who</b> Who is responsible?	<b>Duration</b> How long will it take to complete?	<b>Status</b> Has the task been completed?	
1 Get rough gondola design ideas	Brainstorm based off of literature review	Alex, Sawyer	6 Hours	No	
2 Get quote for keel	Put rough 3D out for quotes	Sawyer	1 Hour	Yes	
3 Get rough dimensions and weights of equipment needed	Find the required components data sheets	Joey, Isaak	6 Hours	No	
4					
5					
<b>Next meeting</b> Chairperson: Isaak Goldenberg	<b>Minute taker:</b> Isaak Goldenberg	<b>Date &amp; Time:</b> 8:30am 20-Sept-2017	<b>Venue:</b> CBY C011		

Group Minutes					
<b>Attendees:</b> Isaak Goldenbergberg igold093@uottawa.ca, Joey Kane jkane035@uottawa.ca, Alex Pennel apenn095@uottawa.ca, Sawyer Woodside swood079@uottawa.ca		<b>Absent:</b>	<b>Date &amp; Time:</b> Sunday, Sept 24th	<b>Venue:</b> Site	
<b>Minute taker:</b> Who is filling out this form?		<b>Chairperson:</b> Who is organising the meeting?			
<b>Task</b> What has to be done?	<b>Action</b> What action is required to get it done?	<b>Who</b> Who is responsible?	<b>Duration</b> How long will it take to complete?	<b>Status</b> Has the task been completed?	
1 Keel desing, Bearing mounting and Batteries selection	Draw sketches of each design concept, being sketches into overleaf file , explain designs	Isaak	2 days		
2 Rack and pinion, position reading, gondola design	Draw sketches of each design concept, being sketches into overleaf file , explain designs	Joey	2 days		
3 friction wheel , communication transmission, timing belt, gondola design	Draw sketches of each design concept, being sketches into overleaf file , explain designs	Alex	2 days		
4 Mounting thrusters to airship, gondola design, keel desing	Draw sketches of each design concept, being sketches into overleaf file , explain designs	Sawyer	2 days		
5					
<b>Next meeting</b> <b>Chairperson:</b> Joey Kane	<b>Minute taker:</b> Joey Kane	<b>Date &amp; Time:</b> Friday, Sept 29th	<b>Venue:</b> CBY		

<b>Group Minutes</b>					
<b>Attendees:</b> Isaak Goldenberg, Igold093@uottawa.ca Joey Kane, JKane035@uottawa.ca Alex Pennell, APenn095@uottawa.ca Sawyer Woodside, SWood079@uottawa.ca		<b>Absent:</b> None		<b>Date &amp; Time:</b> Friday, September 29th, 2017	
<b>Minute taker:</b> Who is filling out this form? Sawyer Woodside		<b>Chairperson:</b> Who is organising the meeting?		<b>Joey Kane</b>	
	<b>Task</b> What has to be done?	<b>Action</b> What action is required to get it done?	<b>Who</b> Who is responsible?	<b>Duration</b> How long will it take to complete?	<b>Status</b> Has the task been completed?
1	Organize and delegate work to all group members	Create an action plan for the modelling report	Joey	1 Hour	Yes
2	Demonstrate final design	Draw sketches of each component in detail	Sawyer	2 Days	No
3	Compute Gondola Reaction Forces	Create free body diagrams and complete static force analysis on gondola parts	Alex	3 Days	No
4	Compute Airship Drag	Create flow simulations in solidworks based on rough dimensions	Joey	2 Days	No
5	Find Thrust Values	Review literature to determine best method of calculating thrust	Isaak	3 Days	No
<b>Next meeting</b> Chairperson: <b>Sawyer Woodside</b>		Minute taker: <b>Sawyer Woodside</b>	Date & Time: Friday, October 6th, 2017	Venue: <b>CBY</b>	

Group Minutes					
<b>Attendees:</b> Isaak Goldenbergberg igold093@uottawa.ca, Joey Kane jkane035@uottawa.ca, Alex Pennel apenn095@uottawa.ca, Sawyer Woodside swood079@uottawa.ca		<b>Absent:</b>	<b>Date &amp; Time:</b> Friday, October 6th	<b>Venue:</b> CBY	
<b>Minute taker:</b> Who is filling out this form?		Sawyer Woodside	<b>Chairperson:</b> Who is organising the meeting?	Sawyer Woodside	
	<b>Task</b> What has to be done?	<b>Action</b> What action is required to get it done?	<b>Who</b> Who is responsible?	<b>Duration</b> How long will it take to complete?	<b>Status</b> Has the task been completed?
1	Gondola Drawings	Draw sketches of each subassembly, how they will be fastened and how they will interact, elaborate in report	Sawyer	5 days	
2	Thruster Support Drawings	Draw sketches of each subassembly, how they will be fastened and how they will interact, elaborate in report	Isaak	5 days	
3	Wiring and Communications	Specify the design, draw sketches of each design concept (wiring diagrams), elaborate in report	Joey and Alex	3 days	
4	Document Tending	Importing Files, formatting, establishing requirements, reworking document template	Alex	2 days	
5					
<b>Next meeting</b> <b>Chairperson:</b> Alex Pennell	<b>Minute taker:</b> Alex Pennell		<b>Date &amp; Time:</b> Friday, October 13th	<b>Venue:</b> CBY	

Group Minutes					
Attendees:		Absent:	Date & Time:	Venue:	
Isaak Goldenberg igold093@uottawa.ca, Joey Kane jkane035@uottawa.ca, Alex Pennel apenn095@uottawa.ca, Sawyer Woodside swood079@uottawa.ca			Thursday, November 2	CBY	
<b>Minute taker:</b> Who is filling out this form?		Isaak Goldenberg	<b>Chairperson:</b> Who is organising the meeting?	Isaak Goldenberg	
	Task What has to be done?	Action What action is required to get it done?	Who Who is responsible?	Duration How long will it take to complete?	Status Has the task been completed?
1	Solve forces on gondola	Code all equations leaving variables adjustable to solve forces acting on gondola	Isaak	5 days	
2	Adjust braking/holding design	Modify braking method in order to not damage and components and ensure efficient braking	All	5 days	
3	Organize Sw files	Begin to set up solid works parts for final design	Sawyer	3 days	
4	Manufacturing method finalizing	Decide on manufacturing methods for each component	Joey	2 days	
5	Set up git hub for coding		Alex	5 days	
<b>Next meeting</b> Chairperson: Isaak Goldenberg		Minute taker: Isaak Goldenberg	Date & Time: Thursday, November 2	Venue: CBY	

<b>Group Minutes</b>					
<b>Attendees:</b> Isaak Goldenberg, igold093@uottawa.ca Joey Kane, jkane035@uottawa.ca Sawyer Woodside, swood079@uottawa.ca Alexander Pennell, apenn095@uottawa.ca		<b>Absent:</b> N/A	<b>Date &amp; Time:</b> 8th of November, 2017	<b>Venue:</b> Isaak Goldenberg's Home	
<b>Minute taker:</b> Who is filling out this form? Joey Kane		<b>Chairperson:</b> Who is organising the meeting? Joey Kane			
	<b>Task</b> What has to be done?	<b>Action</b> What action is required to get it done?	<b>Who</b> Who is responsible?	<b>Duration</b> How long will it take to complete?	<b>Status</b> Has the task been completed?
1	Begin design of final solidworks files.	Solidworks parts and assemblies need to be created, equation based	Sawyer	10 days	No
2	Begin parametrization	Create matlab directories, input equations from modelling report	Alex, Isaak	5 days	No
3	Create LaTeX document	Format document and begin writing section	Joey	2 days	No
4	Redo analysis	Redo some section of analysis report, as well as extra analysis as recommended by the TAs	Joey	3 days	No
5					
<b>Next meeting</b> Chairperson: <b>Sawyer Woodside</b>	<b>Minute taker:</b> <b>Joey Kane</b>	<b>Date &amp; Time:</b> November 15th, 10am	<b>Venue:</b> <b>CBY</b>		

Group Minutes					
<b>Attendees:</b> Isaak Goldenberg, igold093@uottawa.ca Joey Kane, JKane035@uottawa.ca Alex Pennell, APenn095@uottawa.ca Sawyer Woodside, SWood079@uottawa.ca		<b>Absent:</b> None	<b>Date &amp; Time:</b> Thursday, November 16th, 2017	<b>Venue:</b> Goldenberg Residence	
<b>Minute taker:</b> Who is filling out this form? Sawyer Woodside		<b>Chairperson:</b> Who is organising the meeting?	Sawyer Woodside		
	<b>Task</b> what has to be done?	<b>Action</b> What action is required to get it done?	<b>Who</b> Who is responsible?	<b>Duration</b> How long will it take to complete?	<b>Status</b> Has the task been completed?
1	Formating document and adding section in LaTex	Coding LaTex document	Joey	8 Hours	No
2	Preliminary Solidworks	Create CAD files and start .txt files	Sawyer	4 Days	No
3	Computing Forces	Complete analysis and code solvers in Matlab	Alex and Isaak	5 Days	No
4	Start GUI	Begin Preliminary GUI	Alex	10 Days	No
5					
<b>Next meeting</b> Chairperson: <b>Alex Pennell</b>	<b>Minute taker:</b> <b>Sawyer Woodside</b>	<b>Date &amp; Time:</b> Friday, November 17th, 2017	<b>Venue:</b> <b>CBY</b>		

<b>Group Minutes</b>					
<b>Attendees:</b> Isaak Goldenberg, igold093@uottawa.ca Joey Kane, JKane035@uottawa.ca Alex Pennell, APenn095@uottawa.ca Sawyer Woodside, SWood079@uottawa.ca		<b>Absent:</b> None		<b>Date &amp; Time:</b> Wednesday, November 22th, 2017	
<b>Minute taker:</b> Who is filling out this form? Alex Pennell		<b>Chairperson:</b> Who is organising the meeting?		<b>Alex Pennell</b>	
	<b>Task</b> What has to be done?	<b>Action</b> What action is required to get it done?	<b>Who</b> Who is responsible?	<b>Duration</b> How long will it take to complete?	<b>Status</b> Has the task been completed?
<b>1</b>	Build the total parameterization outline	Build upon outline from last report	Joey	8 Hours	No
<b>2</b>	Finish	Create CAD files and .txt files	Sawyer	2 Days	No
<b>3</b>	Continue MATLAB code	Complete analysis and code solvers in Matlab	Alex and Isaak	1 Day	No
<b>4</b>	Start GUI	Begin Preliminary GUI	Alex	10 Days	No
<b>5</b>					
<b>Next meeting</b> Chairperson: <b>Alex Pennell</b>	<b>Minute taker:</b> <b>Alex Pennell</b>		<b>Date &amp; Time:</b> Wednesday, November 22th, 2017	<b>Venue:</b> <b>CBY</b>	

Group Minutes					
<b>Attendees:</b> Isaak Goldenbergberg igold093@uottawa.ca, Joey Kane ikane035@uottawa.ca, Alex Pennel apenn095@uottawa.ca, Sawyer Woodside swood079@uottawa.ca		<b>Absent:</b>	<b>Date &amp; Time:</b> Thursday, November 30	<b>Venue:</b> CBY	
<b>Minute taker:</b> Who is filling out this form?		Isaak Goldenberg	<b>Chairperson:</b> Who is organising the meeting?		Isaak Goldenberg
	<b>Task</b> What has to be done?	<b>Action</b> What action is required to get it done?	<b>Who</b> Who is responsible?	<b>Duration</b> How long will it take to complete?	<b>Status</b> Has the task been completed?
1	Analysis	Finish writing Gondola Analysis Section	Isaak	2 days	
2	FINISH REPORT		All	8 days	
3	Proposed Design	Finish writing up proposed design section	Sawyer	2 days	
4	Proposed design	Get all renders for sawyer for proposed design section	Joey	2 days	
5	Analysis	Finish writing up thruster arm analysis	Alex	2 days	
<b>Next meeting</b> Chairperson:		Minute taker: Isaak Goldenberg	Date & Time: Thursday, November 30	Venue: CBY	

<b>Group Minutes</b>					
<b>Attendees:</b> Isaak Goldenberg, igold093@uottawa.ca Joey Kane, JKane035@uottawa.ca Alex Pennell, APenn095@uottawa.ca Sawyer Woodside, SWood079@uottawa.ca		<b>Absent:</b> None	<b>Date &amp; Time:</b> Thursday, December 7th, 2017	<b>Venue:</b> Goldenberg Residence	
<b>Minute taker:</b> N/A Who is filling out this form?		<b>Chairperson:</b> Who is organising the meeting? <b>Joey Kane</b>			
	<b>Task</b> What has to be done?	<b>Action</b> What action is required to get it done?	<b>Who</b> Who is responsible?	<b>Duration</b> How long will it take to complete?	<b>Status</b> Has the task been completed?
<b>1</b>	Report Writing	Complete all required sections of final report	All	5 Days	No
<b>2</b>	Finish Solidworks	Test edge cases and ensure program works correctly	Sawyer	2 Days	No
<b>3</b>	Finish Parametrization outlines	Understand flow of code and create flowcharts	Isaak	1 Day	No
<b>4</b>	Finish GUI	Complete coding and test edge cases	Alex	3 Days	No
<b>5</b>					
<b>Next meeting</b> Chairperson: <b>N/A</b>	Minute taker: <b>N/A</b>		<b>Date &amp; Time:</b> <b>N/A</b>	<b>Venue:</b> <b>N/A</b>	

## F.2 Team-Partner Meeting Minutes

Team/Partner Minutes			
<b>Attendees:</b> Alex Pennell (apenn095@uottawa.ca,7334789) Isaak Goldenberg (igold093@uottawa.ca,7395188) Joey Kane (jkane035@uottawa.ca,7386330) Sawyer Woodside (swood079@uottawa.ca,7158568)	<b>Absent:</b> none	<b>Date &amp; Time:</b> Sept-15-2017	<b>Venue:</b> C011 and lab
<b>Minute taker:</b> Who is filling out this form?		<b>Chairperson:</b> Who is organising the meeting? <b>Eric Lanteigne</b>	
<b>Minutes</b>			
<p>Discussed overview of the project            Wires can cause issues with the system            Need to use propellers, since they are more efficient            Looked at previous designs            Main focus of the project is to design the gondola, other changes to the blimp are extra</p>			
<b>Next meeting</b> Chairperson:	Minute taker:	Date & Time:	Venue:



## **Appendix G: Recommendations for Improving the Course**

lol